Applied Microbiology and Biotechnology (2020) 104:4515–4532
https://doi.org/10.1007/s00253-020-10543-w

METHODS AND PROTOCOLS

Establishment of CRISPR interference in *Methylorubrum extorquens* and application of rapidly mining a new phytoene desaturase involved in carotenoid biosynthesis

Xu-Hua Mo[1] · Hui Zhang[1] · Tian-Min Wang[2] · Chong Zhang[2] · Cong Zhang[1] · Xin-Hui Xing[2] · Song Yang[1,3]

Received: 23 December 2019 / Revised: 2 March 2020 / Accepted: 11 March 2020 / Published online: 25 March 2020

Abstract

The methylotrophic bacterium *Methylorubrum extorquens* AM1 holds a great potential of a microbial cell factory in producing high value chemicals with methanol as the sole carbon and energy source. However, many gene functions remain unknown, hampering further rewiring of metabolic networks. Clustered regularly interspaced short palindromic repeat interference (CRISPRi) has been demonstrated to be a robust tool for gene knockdown in diverse organisms. In this study, we developed an efficient CRISPRi system through optimizing the promoter strength of *Streptococcus pyogenes*–derived deactivated *cas9* (*dcas9*). When the *dcas9* and sgRNA were respectively controlled by medium $P_{R/tetO}$ and strong $P_{mxaF\text{-}g}$ promoters, dynamic repression efficacy of cell growth through disturbing a central metabolism gene *glyA* was achieved from 41.9 to 96.6% dependent on the sgRNA targeting sites. Furthermore, the optimized CRISPRi system was shown to effectively decrease the abundance of exogenous fluorescent protein gene *mCherry* over 50% and to reduce the expression of phytoene desaturase gene *crtI* by 97.7%. We then used CRISPRi technology combined with 26 sgRNAs pool to rapidly discover a new phytoene desaturase gene *META1_3670* from 2470 recombinant mutants. The gene function was further verified through gene deletion and complementation as well as phylogenetic tree analysis. In addition, we applied CRISPRi to repress the transcriptional level of squalene-hopene cyclase gene *shc* involved in hopanoid biosynthesis by 64.9%, which resulted in enhancing 1.9-fold higher of carotenoid production without defective cell growth. Thus, the CRISPRi system developed here provides a useful tool in mining functional gene of *M. extorquens* as well as in biotechnology for producing high-valued chemicals from methanol.

Key points

- *Developing an efficient CRISPRi to knockdown gene expression in C1-utilizing bacteria*
- *CRISPRi combined with sgRNAs pool to rapidly discover a new phytoene desaturase gene*
- *Improvement of carotenoid production by repressing a competitive pathway*

Keywords *Methylorubrum extorquens* · CRISPRi · sgRNAs pool · Phytoene desaturase · Carotenoid · Gene knockdown

Xu-Hua Mo and Hui Zhang contributed equally to this work.

Electronic supplementary material The online version of this article (https://doi.org/10.1007/s00253-020-10543-w) contains supplementary material, which is available to authorized users.

✉ Song Yang
yangsong1209@163.com

[1] School of Life Sciences, Shandong Province Key Laboratory of Applied Mycology, and Qingdao International Center on Microbes Utilizing Biogas, Qingdao Agricultural University, Qingdao, Shandong Province, People's Republic of China

[2] Department of Chemical Engineering, Tsinghua University, Beijing, People's Republic of China

[3] Key Laboratory of Systems Bioengineering, Ministry of Education, Tianjin University, Tianjin, People's Republic of China

Introduction

Methylorubrum extorquens AM1 (formerly *Methylobacterium extorquens* AM1), a pink-pigment and facultative methylotroph α-proteobacterium, is one representative of methylotrophs that are capable of growing on one-carbon compounds such as methanol or methylamine as the sole carbon and energy source (Peel and Quayle 1961). The genome of the *M. extorquens* AM1 contains one chromosome, one megaplasmid and three plasmids, harboring a total of nearly 6800 genes (Vuilleumier et al. 2009). Recently, much effort has been devoted to elucidating the gene functions, metabolic networks as well as its regulatory mechanisms (Nayak et al. 2016; Ochsner et al. 2017; Ueoka et al. 2018). For one-carbon metabolism, Nayak et al. disclosed the metabolic routes and regulatory network for methylamine oxidation of *M. extorquens* AM1 in different concentrations of methylamine (Nayak et al. 2016), and Ochsner et al. identified almost 100 new methylotrophic genes and elucidated an important regulatory mechanism of the serine cycle using TnSeq method (Ochsner et al. 2017). For secondary metabolism, Ueoka et al. discovered a new *trans*-acyltransferase polyketide biosynthetic gene cluster for synthesizing the antibiotic toblerol by genome mining (Ueoka et al. 2018). Currently, gene knockout through sucrose counterselection is still the most used approach to investigate the gene function in *M. extorquens* AM1 (Marx 2008); however, for rapidly investigating unknown genes, it is still laborious and time-consuming. Transposon mutation has been also developed to screen for gene-phenotype associations or genetic interactions across different environments (Ochsner et al. 2017; Van Dien et al. 2003). One limitation for this technology is that transposon elements insert into the chromosome randomly, making this inappropriate for investigating the targeted gene from the pooled putative genes. Therefore, it is urgent to develop more efficient genetic tools to identify the unknown genes associated with cell phenotypes.

The CRISPR interference (CRISPRi) system has been developed for gene repression in diverse organisms by creating a nuclease-null *Streptococcus pyogenes* Cas9 (deactivated Cas9, or dCas9) in which two inactive mutations of D10A and H840A have been introduced into its RuvC1 and HNH nuclease domains (Larson et al. 2013; Qi et al. 2013; Du et al. 2017; Choudhary et al. 2015; Bruder et al. 2016; Huang et al. 2016; Wang et al. 2019; Hogan et al. 2019; Zhan et al. 2019; Caro et al. 2019). This technology can also be applied as an efficient tool in systematically manipulating transcription of endogenous genes, enabling rapid discovery of new functional genes using pooled sgRNAs (Gilbert et al. 2014; Wang et al. 2018; Lee et al. 2019). Moreover, since the intermediate metabolites serving as the main precursors for biosynthetic pathways are also key metabolites for cell growth, deletion of the genes responsible for core metabolism usually significantly impacts the physiological biochemistry of cells. Therefore, CRISPRi has been applied to fine-tune expression of essential genes with fewer effects of cell phenotype, making it a more favorable tool for manipulating metabolic flux distribution to the desired pathway (Cleto et al. 2016; Lv et al. 2015; Park et al. 2018; Westbrook et al. 2018; Woolston et al. 2018; Tian et al. 2019). For example, Cleto et al. interfered with the expression of *pck* or *pyk* by CRISPRi to achieve a 2- to 3-fold higher titer of L-glutamate, exceeding that in *pck* and *pyk* deletion strains, with the entire process only requiring 3 days (Cleto et al. 2016). In *M. extorquens*, three interlocked metabolic cycles are important for one-carbon assimilation: the serine cycle, the ethylmalonyl-CoA (EMC) pathway, and the poly-3-hydroxybutyrate (PHB) cycle (Zhang et al. 2019). It has been shown that metabolic flux goes through the serine cycle and EMC pathway when cells are grown on methanol, generating a supply of pyruvate and acetoacetyl-CoA, which could be employed as the precursors for production of value-added terpenoids (Van Dien et al. 2003; Zhang et al. 2019). Moreover, previous reports demonstrated to utilize acetyl-CoA and crotonyl-CoA as the precursors to produce mevalonate (Liang et al. 2017), 3-hydroxypropionic acid (Yang et al. 2017), 1-butanol as well as butadiene (Hu et al. 2016; Yang et al. 2018), all of which must be carefully balanced between growth maintenance and product biosynthesis in engineered *M. extorquens*. However, the lack of efficient tools of gene knockdown impedes its further development as a chemicals-production platform.

Just recently the CRISPR-Cas9 genome editing system was developed in methanotrophic bacteria *Methylococcus capsulatus* Bath (Tapscott et al. 2019), and the CRISPRi system was established in the methylotrophic thermophile *Bacillus methanolicus* MGA3 (Schultenkämper et al. 2019). However, considering the specificity and difference of genetic elements (e.g., promoter strength and initial replicon of expression plasmids), a CRISPRi system tailored to the strain is required to modify gene expression in the model methylotroph *M. extorquens*. Herein, we developed the CRISPRi system to effectively knockdown exogenous and endogenous genes in *M. extorquens*, and further application of CRISPRi system led us to identify a new phytoene desaturase involved in carotenoid biosynthesis. In addition, we also validated the usefulness of CRISPRi system in modulating the production of carotenoid via an interrupting competing pathway. The developed CRISPRi system provides a convenient tool in rapidly mining gene functions as well as pathway engineering for production of high value chemicals in *M. extorquens*.

Table 1 Strains and plasmids used in this study

Plasmids/strains	Description	Sources
Plasmids		
pCM80	vector used for gene expression in *M. extorquens*; promoter, P_{mxaF}; antibiotics, Tet^R, Km^R	Marx and Lidstrom (2001)
pLC291	vector used for gene expression in *M. extorquens*; promoter, inducible $P_{R/tetO}$; antibiotics, Km^R	Chubiz et al. (2013)
pCM433	sacB-based allelic exchange vector; antibiotics, Ap^R, Cm^R, Tet^R	Marx (2008)
pAIS	pCM80 derivative contained *dcas9* and sgRNA expression cassette; *dcas9* and sgRNA under the control of constitutive promoter P_{mxaF} and $P_{mxaF\text{-}g}$ respectively	This study
pAIM	pCM80 derivative contained *dcas9* and sgRNA expression cassette; *dcas9* and sgRNA under the control of constitutive promoter P_{coxB} and $P_{mxaF\text{-}g}$ respectively	This study
pAIW	pCM80 derivative with *dcas9* and sgRNA expression cassette; *dcas9* and sgRNA under the control of constitutive promoter P_{fumC} and $P_{mxaF\text{-}g}$ respectively	This study
pAIL	pCM80 derivative with *dcas9* and sgRNA expression cassette; *dcas9* and sgRNA under the control of constitutive promoter P_{lac} and $P_{mxaF\text{-}g}$, respectively	This study
pAIO	pCM80 derivative with *dcas9* and sgRNA expression cassette; *dcas9* and sgRNA under the control of inducible promoter $P_{R/tetO}$ and $P_{mxaF\text{-}g}$, respectively	This study
pAIR	pAIO harbors the repressor TetR for $P_{R/tetO}$	This study
pACR	pCM80 derivative with overexpression of *META1_3670* under the control of P_{mxaF}; antibiotics, Tet^R	This study
pAIF	pCM433 with gene fragments of *glmS*, P_{mxaF}-*mCherry* and *META1_4547*; antibiotics, Ap^R, Cm^R, Tet^R	This study
pAIP	pCM433 with 1 kb upstream and 1 kb downstream fragments of *META1_3670*; antibiotics, Ap^R, Cm^R, Tet^R	This study
pAIB	pCM433 with 1 kb upstream and 1 kb downstream fragments of *crtB*; antibiotics, Ap^R, Cm^R, Tet^R	This study
Strains		
E. coli DH5α	F recA1 endA1 thi-1 *hsdR*17 supE44 relA1deoR(lacZYA-argF) U169 80dlacZM15	Lab storage
M. extorquens AM1	Wild-type, pink color, rifamycin-resistant strain	Nunn et al. (1986)
YA	*M. extorquens* AM1::pCM80	Lab storage
YAIM	*M. extorquens* AM1::P_{mxaF}-*mCherry*	This work
YAIP	*M. extorquens* AM1::Δ*META1_3670*	This work
YACR	YAIP carrying the plasmid pACR	This work
YAIB	*M. extorquens* AM1::Δ*crtB*	This work
YMZA-1 to 4	*M. extorquens* AM1 carrying the plasmids pAIS-*glyA*-(NT0, NT41, NT571 and NT691)	This work
YMZA-5 to 8	*M. extorquens* AM1 carrying the plasmids pAIL-*glyA*-(NT0, NT41, NT571 and NT691)	This work
YMZA-9 to 12	*M. extorquens* AM1 carrying the plasmids pAIW-*glyA*-(NT0, NT41, NT571 and NT691)	This work
YMZA-13 to 16	*M. extorquens* AM1 carrying the plasmids pAIM-*glyA*-(NT0, NT41, NT571 and NT691)	This work
YMZA-17 to 20	*M. extorquens* AM1 carrying the plasmids pAIO-*glyA*-(NT0, NT41, NT571 and NT691)	This work
YMZA-21 and 23	*M. extorquens* AM1 carrying the plasmids pAIO-*crtI* (*META1_3665*)-(NT6, NT212 and NT1168)	This work
YMZA-24 to 26	*M. extorquens* AM1 carrying the plasmids pAIO- *META1_3670*-(NT29, NT815 and NT1500)	This work
YMZA-27 to 29	*M. extorquens* AM1 carrying the plasmids pAIO-*shc*-(NT14, NT1017 and NT1956)	This work
YAIM-1 to 6	YAIM carrying the plasmids pAIF-*mCherry* -(NT0, NT32, NT77, NT483 and NT641); YAIM 6 carrying the plasmids pAIR-*mCherry*-NT77	This work

Materials and methods

Strains, media, and culture conditions

The plasmids and strains used in this study are listed in Table 1. All *Escherichia coli* strains were cultured in Luria-Bertani (LB) agar or liquid medium at 37 °C supplemented with antibiotics where necessary at a final concentration of 20 μg/ml tetracycline (Tet) or 25 μg/ml kanamycin (Km). *M. extorquens* AM1 ATCC 14718 and the derivative strains were routinely cultured in a minimal medium at 30 °C as described previously (Yang et al. 2017). Substrates and antibiotics were supplied at the following concentrations: methanol (125 mM) or succinate (15 mM) as the sole carbon source. All chemicals used in media were purchased from Sigma-Aldrich (St. Louis, MO, USA) unless otherwise specified.

Table 2 Primers and sgRNAs used in this study

Primers	Sequences (5′-3′)	Usage
$P_{mxaF\text{-}g}$-1F	CCCGCTTGGTCGGGCCGCTTC	Construction of pgRNA
$P_{mxaF\text{-}g}$-1R	TCACGACGTTGTAAAACGACG	Construction of pgRNA
P_{mxaF}-F	CTTGCATGCCTGCAGGTCGACTCTAGATCCCG CTTGGTCGGGCCGCTT	Construction of pAIS
P_{mxaF}-R	ATTGAGTATTTCTTGTCCATGGCGTAATCATGGTCATA GCTGTTTCCT	Construction of pAIS
P_{mxaF}-dCas9-F	AGGAAACAGCTATGACCATGATTACGCCATGG ACAAGAAATACTCAAT	Construction of pAIS
$P_{R/tetO}$-F	CTTGCATGCCTGCAGGTCGACTCTAGACAACA ACTTATACCATGGCC	Construction of pAIO
$P_{R/tetO}$-R	ATTGAGTATTTCTTGTCCATTCTCTATCACTGATAGGG ATTAC	Construction of pAIO
$P_{R/tetO}$-dCas9-F	GTAATCCCTATCAGTGATAGAGAATGGACAAG AAATACTCAAT	Construction of pAIO
P_{fumC}-F	CTTGCATGCCTGCAGGTCGACTCTAGACGTGA GCGGCGGCGGCACCT	Construction of pAIW
P_{fumC}-R	ATTGAGTATTTCTTGTCCATCATCGTGGCCTCTTCGTT GGCTC	Construction of pAIW
P_{fumC}-dCas9-F	GAGCCAACGAAGAGGCCACGATGATGGACAAG AAATACTCAAT	Construction of pAIW
P_{coxB}-F	CTTGCATGCCTGCAGGTCGACTCTAGACGTAT CCCCAGAGGCAGCCA	Construction of pAIM
P_{coxB}-R	ATTGAGTATTTCTTGTCCATCATGTCCCCGCTTGGCTC CCCT	Construction of pAIM
P_{coxB}-dCas9-F	AGGGGAGCCAAGCGGGGACATGATGGACAAGA AATACTCAAT	Construction of pAIM
P_{lac}-F	CTTGCATGCCTGCAGGTCGACTCTAGATTTACACTTTA TGCTTCCGG	Construction of pAIL
P_{lac}-R	ATTGAGTATTTCTTGTCCATATTGTTATCCGCTCACAA TTC	Construction of pAIL
P_{lac}-dCas9-F	GAATTGTGAGCGGATAACAATATGGACAAGAA ATACTCAAT	Construction of pAIL
HR-F	GAAGCGGAAGAGCGCCCAATAC	Verification of pAIS, pAIO, pAIW, pAIM, pAIL
dCas9-R	CGTTGTAAAACGACGGCCAGTGAATTCTCAGT CGCCGCCGAGCTGCGACAGGTCG	Construction and Verification of pAIS, pAIO, pAIW, pAIM, pAIL
glyA-NT41-F	TCAAAGCCTAGAAAATATAGGGCAAGATGAGCCG AGAAGAGTTTTAGAGCTAGAAATAG	Construction of pAIS/pAIM/pAIW/pAIL/ pAIO-*glyA*-NT41, underline is the sequence targeting *glyA*
glyA-NT571-F	TCAAAGCCTAGAAAATATAGTTCGCGAAGTCCCA GTGACGGTTTTAGAGCTAGAAATAG	Construction of pAIS/pAIM/pAIW/pAIL/ pAIO-*glyA*-NT571, underline is the sequence targeting *glyA*
glyA-NT691-F	TCAAAGCCTAGAAAATATAGGTGGTGGCGACGTG CGCGTGGTTTTAGAGCTAGAAATAG	Construction of pAIS/pAIM/pAIW/pAIL/ pAIO-*glyA*-NT691, underline is the sequence targeting *glyA*
mCherry-NT32-F	TCAAAGCCTAGAAAATATAGGCGCATGAACTCCT TGATGAGTTTTAGAGCTAGAAATAG	Construction of pAIO-*mCherry*-NT32, underline is the sequence targeting *mCherry*
mCherry-NT77-F	TCAAAGCCTAGAAAATATAGCTCGAACTCGTGGC CGTTCAGTTTTAGAGCTAGAAATAG	Construction of pAIO-*mCherry*-NT77, underline is the sequence targeting *mCherry*
mCherry-NT590-F	TCAAAGCCTAGAAAATATAGCAACTTGATGTTGA CGTTGTGTTTTAGAGCTAGAAATAG	Construction of pAIO-*mCherry*-NT590, underline is the sequence targeting *mCherry*
mCherry-NT641-F	TCAAAGCCTAGAAAATATAGTCGTGGAACAGTAC GAACGCGTTTTAGAGCTAGAAATAG	Construction of pAIO-*mCherry*-NT641, underline is the sequence targeting *mCherry*
crtI -NT6-F	TCAAAGCCTAGAAAATATAGCGACCGCGACCGAA GAACCCGTTTTAGAGCTAGAAATAG	Construction of pAIO-*crtI*-NT6, underline is the sequence targeting *crtI*
crtI -NT212-F	TCAAAGCCTAGAAAATATAGGTGCACCGAGCGCC CGGCCTGTTTTAGAGCTAGAAATAG	Construction of pAIO-*crtI*-NT212, underline is the sequence targeting *crtI*
crtI -NT1168-F	TCAAAGCCTAGAAAATATAGATCTTCGACCAGTC GTGATGGTTTTAGAGCTAGAAATAG	Construction of pAIO-*crtI*-NT1168, underline is the sequence targeting *crtI*
META1_ 3670-NT29-F	TCAAAGCCTAGAAAATATAGGATCGTGCGGCGGC CCGACAGTTTTAGAGCTAGAAATAG	Construction of pAIO-*META1_3670*-NT29, underline is the sequence targeting *META1_3670*

Table 2 (continued)

Primers	Sequences (5′-3′)	Usage
META1_3670-NT815-F	TCAAAGCCTAGAAAATATAGGCCGCCGACGAACACGCCGGGTTTTAGAGCTAGAAATAG	Construction of pAIO-*META1_3670*-NT815, underline is the sequence targeting *META1_3670*
META1_3670-NT1500-F	TCAAAGCCTAGAAAATATAGCCTTGGCGAGATCCTCGATCGTTTTAGAGCTAGAAATAG	Construction of pAIO-*META1_3670*-NT1500, underline is the sequence targeting *META1_3670*
Com-R	CTATATTTTCTAGGCTTTGATTG	Construction of pAIS, pAIO, pAIW, pAIM, pAIL targeting different gene and site
Upstream-F Downstream-R	GAGCGGATAACAATTTCACACAG GACCTTGGCCATCTCGTTC	Primers for amplification of fragments contained sgRNAs

Construction of CRISPRi plasmids and recombinant *M. extorquens* strains

The primers used in this study are listed in Table 2 and Table S1. The codons for the *S. pyogenes dcas9* were optimized according to *M. extorquens* AM1 codon preferences (Yang et al. 2017), and the sequences for *dcas9* (GenBank accession number is MN896903) were synthesized by Sangon Biotech Co. Ltd. (Shanghai, China). The sgRNAs were designed by using Python software package (Guo et al. 2018). Each sgRNA biobrick contained three parts: a 20-bp DNA region complementing the gene sequence of interest called the based-pairing region (BPR), a 42-bp hairpin region for dCas9 protein binding termed dCas9 handle (DH), and a 40-bp terminator *rrnB*. The sequences containing $P_{mxaF\text{-}g}$-sgRNA-dcas9 handle-*rrnB* were synthesized by Sangon Biotech Co. Ltd. (Shanghai, China). The pCM80 plasmid was used as the parent plasmid for developing the CRISPRi system. We amplified $P_{mxaF\text{-}g}$ and sgRNA by primers of $P_{mxaF\text{-}g}$-1F and $P_{mxaF\text{-}g}$-1R to replace the original P_{mxaF} on pCM80 to obtain the plasmid pgRNA. After *dcas9* amplified by primers of P_{mxaF}-dCas9-F and dCas9-R as well as promoter P_{mxaF} amplified by primers of P_{mxaF}-F and P_{mxaF}-R, the cassette "P_{mxaF}-*dcas9*" was amplified by PCR using primers of P_{mxaF}-F and dCas9-R with *dcas9* fragment and promoter P_{mxaF} as template. The P_{mxaF}-*dcas9* cassette was cloned into plasmid pgRNA digested with restriction enzymes *Sac*I and *Bam*HI by using ClonExpress®II One Step Cloning Kit (Vazyme Biotech Co. Ltd., Nanjing, China) and transformed into *E. coli* DH5α to confer the plasmid pAIS. The promoters of P_{coxB} and P_{fumC} amplified from *M. extorquens* AM1, P_{lac} amplified from pCM80, and $P_{R/tetO}$ amplified from pLC291 were respectively used to construct the plasmids pAIM, pAIW, pAIL, and pAIO as described above.

By using reverse PCR technology with the primers containing the 20-bp DNA region complementing the targeting gene sequence as reported (Van Dien et al. 2003), three plasmids pAIM-*glyA*-NT41, pAIM-*glyA*-NT571, and pAIM-*glyA*-NT691 that contained the sgRNAs targeting different regions of the non-template strand of *glyA* gene were constructed. The constructed plasmids were introduced into *M. extorquens* AM1 by electroporation, and then, the recombinant strains were cultured in the medium containing succinate as the sole carbon and energy source, leading to afford YMZA-2, YMZA-3, and YMZA-4, respectively. Similar to the strains of YMZA-2 to YMZA-4, the strains of YMZA-5 to YMZA-8, YMZA-9 to YMZA-12, YMZA-13 to YMZA-16, and YMZA-17 to YMZA-20 were obtained as described above.

To interfere the phytoene desaturase gene *crtI* (*META1_3665*) and squalene-hopene cyclase gene *shc*, three sgRNAs targeting different regions of the non-template strand of coding sequence were designed for each gene. By using reverse PCR technology with plasmid pAIO as template, six plasmids (pAIO-*crtI*-NT6, pAIO-*crtI*-NT212 and pAIO-*crtI*-NT1168 for targeting *crtI*, pAIO-*shc*-NT14, pAIO-*shc*-NT1017 and pAIO-*shc*-NT1956 for targeting *shc*) were constructed, which were introduced into *M. extorquens* AM1 to create the strains YMZA-21 to YMZA-23 and YMZA-27 to YMZA-29, respectively.

Interference of red fluorescence protein gene *mCherry*

The red fluorescence protein gene *mCherry* was inserted into the chromosome of *M. extorquens* AM1 between *glmS* and *META1_4547* using the method described previously (Marx 2008). Briefly, after amplification of genes *glmS* and *META1_4547* from *M. extorquens* AM1 and P_{mxaF}-*mCherry* cassette from plasmid pSWU-*mCherry* (constructed by our Lab), then, the three fragments were overlapped by PCR to generate *glmS*-P_{mxaF}-*mCherry*-*META1_4547*, which was further digested by *Bgl*II and *Sac*I and cloned into pCM433 to afford plasmid pAIF. The pAIF was then electroporated into the wild-type *M. extorquens* AM1. *M. extorquens* AM1 bearing pAIF was firstly selected by using tetracycline resistance phenotype, and double-crossover mutants occurred by growing on the plates containing 5% sucrose (w/v). The mutant strain with successful allele swapping was confirmed by PCR with primers of genome-*glmS*-F and genome-1199-R, and the PCR fragment with expected size was further sequenced. The mutant strain with correct P_{mxaF}-*mCherry* cassette was termed as YAIM.

Five sgRNAs targeting the different region of the non-template strand of *mCherry* were designed. The plasmids pAIO-NT0, pAIO-*mCherry*-NT32, pAIO-*mCherry*-NT77, pAIO-*mCherry*-NT483, and pAIO-*mCherry*-NT641 for interfering with *mCherry* were constructed by using reverse PCR with plasmid pAIO-NT0 as template, which were then introduced into the YAIM strain to generate the strains of YAIM-1 to YAIM-5. The interference efficacy toward *mCherry* was evaluated by determining the fluorescent value. The strains of YAIM-1, YAIM-2, YAIM-3, YAIM-4, and YAIM-5 were inoculated into the tubes and grown to OD_{600} with about 0.8. Then, 1.2 ml cells were transferred into 250 ml flasks with 50 ml fresh medium to obtain the initial OD_{600} with 0.02. The cells were cultured on rotary shaker at 200 rpm at 30 °C. When the OD_{600} reached about 1.0, 200 μl cells were transferred into a 96-well plate and the fluorescence intensity were measured by Cytation1 imaging reader (BioTek, Winooski, VT, USA) under the instruction of the protocol. Relative fluorescence values reported here are as follows:

Relative fluorescence $(\mathrm{A.U.}) = \frac{\mathrm{RFU}}{\mathrm{OD}_{600}} \times 10^{-3}$, A.U. means arbitrary units, and RFU means red fluorescence unit.

Data were expressed as means ± standard deviations of results from three biological replicates.

Measurement of growth of *M. extorquens* and recombinant strains

M. extorquens and its recombinant strains were initially inoculated into the tubes containing 3 ml medium with 15 mM succinate as the sole carbon source. For each strain, three biological parallels were prepared. When the strains were grown to the middle exponential phase with OD_{600} value of about 0.8, the cells were harvested, and the supernatants were discarded. Then, the pellets were resuspended, and 1.2 ml cell culture was transferred into 250-ml flask with 50-ml minimal medium to obtain the initial OD_{600} of 0.02 and then grown on rotary shaker at 200 rpm at 30 °C for further monitoring growth curve. For each time point, a 0.5-ml sample was taken for OD_{600} measurement by using UV-visible spectrophotometer (Genesys10S, CA, USA). The growth rates presented here represent the mean plus standard deviations calculated from triplicate biological replicates. The specific growth rates were determined by fitting an exponential growth model using Curve Fitter software (Harcombe et al. 2016; http://www.evolvedmicrobe.com/Software.html).

RNA isolation and RT-qPCR analysis

When *M. extorquens* AM1 and the recombinants were grown to the exponential phase with OD_{600} value of about 0.8 in a minimal medium using methanol as the sole carbon source, 1 ml aliquots of each culture were taken and centrifuged (10,000×*g*, 1 min). The pellets were immediately frozen in liquid nitrogen and were stored at − 80 °C until further RNA isolation. The cells were lysed by resuspension of pellets in 1 ml TozolUP buffer (TransGen Biotech, China), 200 μl chloroform, and bead beating for 4 × 90 s with intermittent cooling on ice in Bioprep-6 biological sample homogenizer (All For Life Science Co. Ltd., Hangzhou, China). The RNase-free steel beads used here were 0.3 mm in diameter. The total RNA was extracted by using TransZol Up RNAspin Mini Kit (TransGen Biotech, Beijing, China) according to the instruction of protocol. The residual DNA in the extracted RNA sample was digested by DNaseI (Vazyme Biotech Co. Ltd., Nanjing, China). For each strain, the RNA was isolated from three biological replicates. The RNA degradation and contamination were checked on 1% agarose gels. Quality and quantity of RNA were determined by using spectrophotometer Nano Drop 1000 (Thermo Fisher Scientific, MA, USA).

One thousand nanograms of RNA was reversely transcribed to cDNA by using HiScript® IIQRT SuperMix kit for qPCR (Vazyme Biotech Co. Ltd., Nanjing, China). The real-time RT-qPCR was performed with AceQ Universal SYBR qPCR Master Mix (Vazyme Biotech Co. Ltd., Nanjing, China) by using an ABI 7500 (QuantStudio 5, Thermo Fisher Scientific, MA, USA) instrument equipped with step two real-time system (Applied Biosystems, MA, USA). The gene *rpsB* encoding for 30S ribosomal protein S2 was employed as a reference gene (Chou et al. 2009). RT-qPCR was performed in accordance with the manufacturer's instructions. Each reaction was conducted in three replicates. The relative quantification for RT-qPCR experiments was analyzed by $2^{-\Delta\Delta Ct}$ method (Chou et al. 2009; Chou and Marx 2012). The Ct values obtained were used as the original data to calculate the relative transcriptional expression level of the candidate genes normalized against that of 30S ribosomal protein S2 gene.

Mining unknown genes involved in biosynthesis of carotenoid

Blastp analysis of *M. extorquens* AM1 proteome by using identified phytoene desaturase (*crtI*, *META1_3665*) and annotated phytoene synthase (*crtB*, *META1_3220*) revealed homologous phytoene desaturase genes (*META1_2923*, *META1_3219*, *META1_3670*, and *META1_3679*) and terpene/phytoene synthase (*META1_4618*, *META1_1815*, *META1_1816*, and *META1_3220*) in *M. extorquens* AM1 genome. For each gene, three sgRNAs targeting the front, middle, and terminal region of coding sequences were designed. The primers targeting phytoene desaturase genes (*META1_2923*, *META1_3219*, *META1_3670*, *META1_3679*, *META1_3665*) were mixed in equal concentration, and the

primers targeting terpene/phytoene synthase (*META1_4618*, *META1_1815*, *META1_1816*, and *META1_3220*) were also mixed in equal concentration. By using reverse PCR with plasmid pAIO-NT0 as template and mixed primers, followed by *Dpn*I digestion template, the PCR fragments were recovered from gel and introduced into *E. coli* DH5α competent cells to afford two pools that the plasmids carried all related sgRNAs. All the transformants on the plate were washed into flasks for overnight culture, and the plasmids were extracted and introduced into *M. extorquens* AM1 by electroporation. By this method, two *M. extorquens* AM1 recombinant libraries carrying different plasmids for CRIPSRi were developed. For the recombinants carrying plasmids targeting phytoene desaturase genes, 50 faint pink or colorless recombinant strains were randomly picked up, and the sgRNA regions of the plasmids were amplified by PCR with the primers of upstream-F and downstream-R for further sequencing.

For verifying the gene functions, the phytoene desaturase gene *META1_3670* and phytoene synthase gene *META1_3220* were respectively deleted by using the similar approach as the gene *mCherry* integration described above. For the mutant strain YAIP lacking *META1_3670*, the complementary experiment was conducted. The *META1_3670* was amplified and cloned into pCM80 under promoter P_{mxaF} to afford the plasmid pACR, which was then electroporated into the strain YAIP to perform the YACR strain.

Extraction and analysis of carotenoid

The carotenoid was extracted from *M. extorquens* AM1 as described previously (Van Dien et al. 2003; Tian et al. 2019). The extracts from 50 ml of cell culture was dissolved in 0.1 ml of DMSO, and 30 μl was subject to HPLC analysis by using Waters HPLC 1260 (Waters, MA, USA) equipped with a Waters Spherisorb 5.0 μm ODS2 (4.6 mm × 250 mm, 5 μm) column. The mobile phases were consisting of acetonitrile-water (solvent A, 9:1, V/V) and methanol-isopropanol (solvent B, 3:2, V/V). The elution program was set as follows: 100% A to 5% A in 0–10 min, 5% A retained from 10 to 20 min, and 5% A to 100% A in 20 to 25 min. The flow rate was 1.0 ml/min, and the UV absorbance of the peaks was collected from 200 to 600 nm using a photodiode array detector and monitored at 460 nm. Absorbance was converted to total carotenoid concentration by comparison to a carotenoid standard calibration curve and normalization to cell dry weight.

Statistical analysis

T test was applied to analyze all quantitative data. For each quantitative experiment, all data represent the averages of at least 3 parallels. $p < 0.05$ was considered as significant, $*p < 0.05$; $**p < 0.01$; $***p < 0.001$.

Results

Construction of a CRISPRi system in *M. extorquens* AM1

The serine hydroxymethyl transferase catalyzing the conversion from glycine plus methylene H_4F to serine is a rate-limited enzyme in the serine cycle, which is required for carbon assimilation from methanol in *M. extorquens* AM1 (Smejkalová et al. 2010). Consequently, its encoding gene *glyA* was chosen as the target for constructing and optimizing the CRISPRi system in this study. We placed sgRNA under a natural strong promoter P_{mxaF} derived from methanol dehydrogenase of *M. extorquens* AM1, as insufficient sgRNA expression has been reported to cause low repression behavior (Schada et al. 2015). Since the mismatch sequence of sgRNAs in the 5′-terminus has demonstrated to critically impact the interference efficiency (Larson et al. 2013), the sequence of P_{mxaF} was then carefully truncated to 190-bp ($P_{mxaF\text{-}g}$) based on the putative transcriptional start site by BPROM software (Fig. S1) (Schada et al. 2015). The GC content of *dcas9* gene derived from *S. pyogenes* (35%) is much lower than that of *M. extorquens* AM1 (68%) (Vuilleumier et al. 2009); thus, we optimized the coding sequences of *S. pyogenes dcas9* according to *M. extorquens* codon preferences (Yang et al. 2017). In addition, because the promoter regions in *M. extorquens* AM1 have not been well characterized yet and a number of reports have shown success with the sgRNA targeting non-template strand of coding sequences in bacteria, yeast, or human cells (Qi et al. 2013; Du et al. 2017; Choudhary et al. 2015; Bruder et al. 2016; Huang et al. 2016; Wang et al. 2019), the non-template strand of *glyA* was selected for further interference. Three sgRNAs were designed to target different coding regions of *glyA* as well as one control sgRNA that did not target the genome of *M. extorquens* AM1. The CRISPRi elements are shown in Fig. 1a, and backbone plasmid pCM80, derived plasmids, and primers for constructing CRISPRi are shown in Tables 1 and 2. To establish an initial test of CRISPRi-mediated *glyA* repression, the plasmids pAIS-*glyA*-NT0, pAIS-*glyA*-NT41, pAIS-*glyA*-NT571, and pAIS-*glyA*-NT691 with P_{mxaF} driving *dcas9* were introduced into *M. extorquens* AM1 by electroporation. The growth curves of the resulting recombinant strains were measured when grown on methanol. Unexpectedly, compared to the control sgRNA (the YMZA-1 strain), the sgRNAs targeting three sites of *glyA* (the strains of YMZA-2, YMZA-3, and YMZA-4) showed no decreased growth rates at all (Fig. 1b). Previous studies have reported the recombinant *M. extorquens* expressing the heterologous genes from a promoter of intermediate strength produced the higher product titer (Rohde et al. 2017), which made us consider that the decrease of transcript levels of *dcas9* might help to generate the effective interference.

Four relatively low activities of promoters (constitutive promoters of P_{coxB}, P_{fumC}, and P_{lac} as well as the inducible promoter $P_{R/tetO}$) were explored to analyze *dcas9* expression (Schada et al. 2015; Chubiz et al. 2013). For the constitutive promoters, previous research has demonstrated that the relative activities are followed by the order of P_{fumC} (5–15%) < P_{coxB} (40–50%) < P_{tuf} (70–100%) ≈ P_{mxaF} (100%) in *M. extorquens* AM1 (Schada et al. 2015). For the inducible promoter, as the maximal inducible level of $P_{R/tetO}$ achieves about 33% of P_{mxaF} activity (Chubiz et al. 2013), at the beginning, this promoter was introduced into pCM80 without its regulatory protein TetR. We then extracted the RNA and evaluated the transcriptional levels of *dcas9* by RT-qPCR (Fig. S2; Fig. 2). As shown in Fig. 2, the mRNA level of *dcas9* driven by P_{coxB} was about 40% lower than that of P_{mxaF} and 3.5-fold and 4.0-fold higher than that of P_{fumC} and P_{lac}. The mRNA level obtained by $P_{R/tetO}$ without TetR was slightly lower than that of P_{coxB}. These results were basically in line with the previously reported activities of promoters (Schada et al. 2015; Chubiz et al. 2013).

Furthermore, we examined the interference efficacy for each recombinant strain. As shown in Fig. 3 a and b, P_{lac} driving *dcas9* did not result in any significant growth repression for three targeting sites NT41, NT571, and NT691, but P_{fumC} could obtain 21.7% of repression efficacy for the site NT691 in the recombinant strain YMZA-12. Moreover, we found that P_{coxB} could reduce the growth rate of the strains of YMZA-14 and YMZA-16 with even higher repression efficacy of 29.3% and 63.5% for the targeting sites NT571 and NT691 (Fig. 3c). Notably for the promoter $P_{R/tetO}$, we were surprised to find that the recombinant strains YMZA-18 to YMZA-20 had very significantly reduced growth rates of 71.1%, 41.9%, and 96.6% for all three targeting sites (Fig. 3d). For more details, after cultured in methanol for about 40 h, the OD_{600} value of the YMZA-18 to YMZA-20 strains were attenuated to 0.11, 0.076, and 0.034 with the specific growth rate of 0.035/h, 0.068/h, and 0.004/h (Fig. 3d). In contrast, the control strain YMZA-17 had already entered stationary phase with the OD_{600} value over 1.60 in the same time period. To further explore if we could obtain a more dynamic range of interference, the regulatory protein TetR was introduced along with $P_{R/tetO}$ to create pAIR. Unfortunately, the highest repression efficacy at different concentrations of inducer anhydrotetracycline (ATc) (10, 20, and 50 ng/ml were added when the cells were inoculated in the cultural medium) was not as effective as that of $P_{R/tetO}$ only on plasmid (data not shown), suggesting that $P_{R/tetO}$ itself could perform as a constitutive promoter transcribing *dcas9* to efficiently interfere with gene expression. Taken together, our results demonstrated that $P_{R/tetO}$ without TetR could achieve dynamic ranges of interference dependent on the targeting sites.

Exploring the feasibility of CRISPRi system in repressing other exogenous and endogenous genes

To explore the feasibility of CRISPRi system developed here, the exogenous gene *mCherry* encoding for the red fluorescent protein and endogenous gene *crtI* involved in carotenoid biosynthetic pathway was interfered respectively. The plasmids with *dcas9* gene driven by $P_{R/tetO}$ without TetR and sgRNAs under control of $P_{mxaF\text{-}g}$ were constructed as shown in Table 1. The *mCherry* cassette under control of promoter P_{mxaF} was firstly integrated into the chromosome between *glmS* and *META1_4547* of *M. extorquens* AM1 through homologous recombination [35]. We imaged recombinant strains and subjected the images to automated analysis to determine the average fluorescence. Compared to the control strain YAIM-1, the YAIM-3 strain showed the highest repression effect with the fluorescence value reduced by 51.3% (Fig. 4), and the following repression efficacy for the strains of YAIM-2, YAIM-4, and YAIM-5 was 37.9%, 25.2%, and 31.3%, respectively. Then, we evaluated the transcriptional level of *mCherry* in the strain of YAIM-3, in which the mRNA of *mcherry* was decreased by 88.0% accordingly (Fig. 4a).

To interfere *crtI* (*META1_3665*) encoding a phytoene desaturase involved in secondary metabolism of pink-pigment carotenoid biosynthesis [7], three plasmids pAIO-c*rtI*-NT6, pAIO-c*rtI*-NT212, and pAIO-c*rtI*-NT1168 targeting different sites of the non-template strand were introduced into *M. extorquens* AM1. Comparing with the control strain YMZA-17, the production of carotenoid was decreased by 89.5%, 25.3%, and 97.7% in the recombinant strains (Fig. 5 a and b). The transcriptional levels of *crtI* were also significantly decreased to 14.3%, 62.5%, and 3.1% of that in native mRNA expression, respectively (Fig. 5b). These results clearly demonstrated that our CRISPRi system was also very efficient for the genes participating in secondary metabolism.

Application of CRISPRi to mine unknown enzymes involved in carotenoid biosynthesis

The essential genes such as *crtB* and *crtI* responsible for carotenoid biosynthesis are usually clustered in the chromosome of bacteria (Fukaya et al. 2018; Sedkova et al. 2005); however, our bioinformatics analysis and previous research revealed that the phytoene desaturase gene *crtI* (*META1_3665*) was not flanked by the possible phytoene synthase gene *crtB* in *M. extorquens* AM1 (Fig. 6a) (Van Dien et al. 2003). Thus, we tried to employ the developed CRISPRi system to rapidly identify other unknown genes possibly participating in synthesizing the carotenoid (Fig. 6b). We mined eight potential genes encoding for four putative phytoene synthases (META1_2923, META1_3219, META1_3670, and META1_3679), one terpene synthase (META1_4618), and

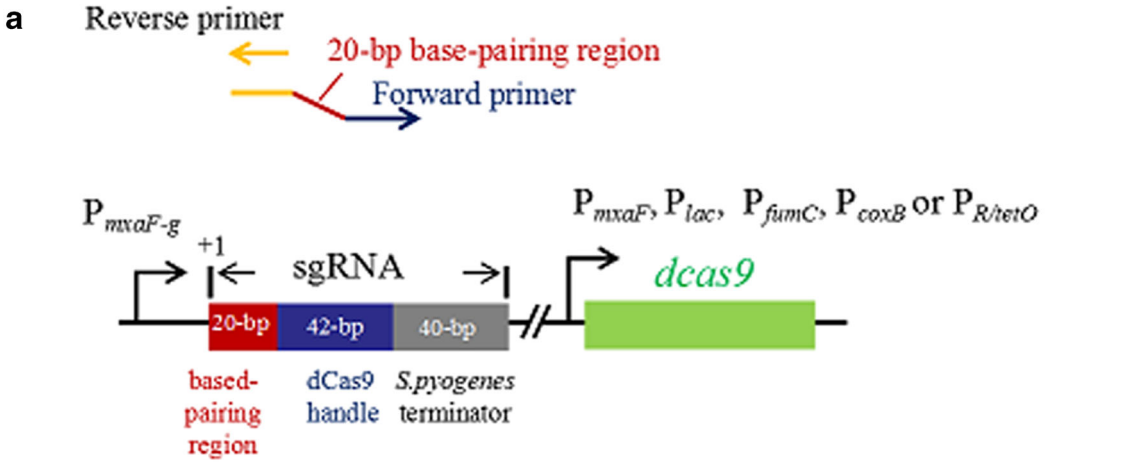

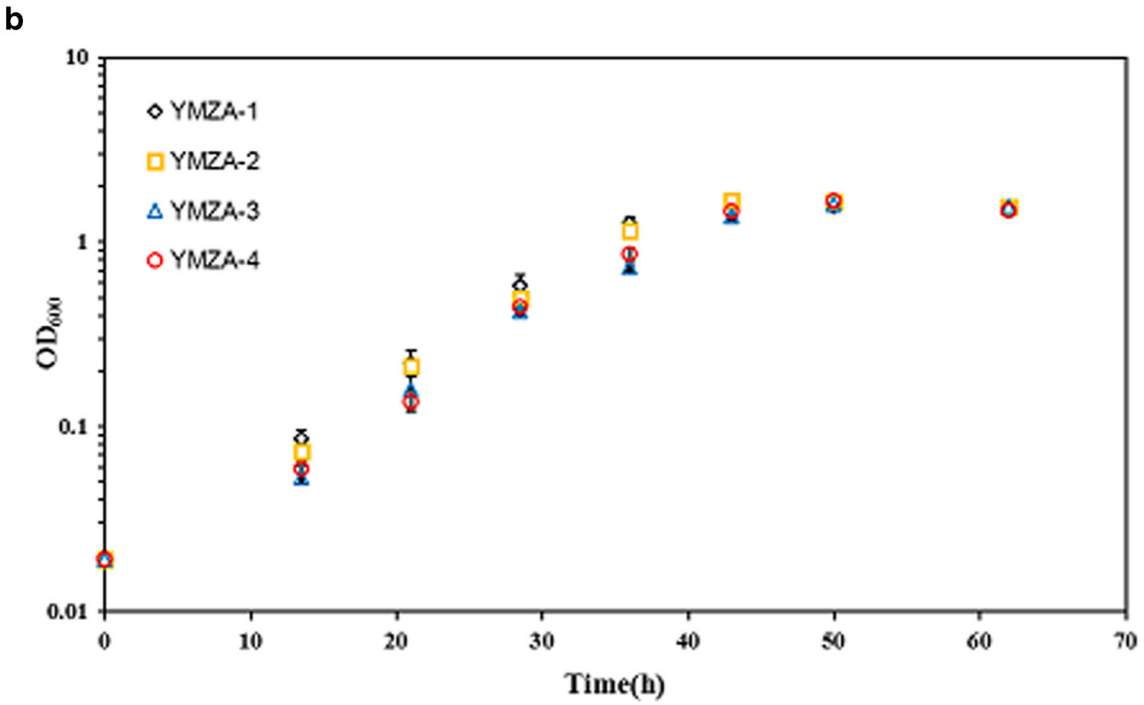

Strains	Specific growth rate (h^{-1})
YMZA-1: *M. extorquens* AM1:: pCM80-P_{mxaF}-*dCas9*-$P_{mxaF\text{-}g}$-*NT0*	0.117 ± 0.007
YMZA-2: *M. extorquens* AM1:: pCM80-P_{mxaF}-*dCas9*-$P_{mxaF\text{-}g}$-*glyA-NT41*	0.112 ± 0.009
YMZA-3: *M. extorquens* AM1:: pCM80-P_{mxaF}-*dCas9*-$P_{mxaF\text{-}g}$-*glyA-NT571*	0.116 ± 0.002
YMZA-4: *M. extorquens* AM1:: pCM80-P_{mxaF}-*dCas9*-$P_{mxaF\text{-}g}$-*glyA-NT691*	0.113 ± 0.005

Fig. 1 Construction of the CRISPRi system in *M. extorquens* AM1. **a** The developed CRISPRi elements. The biobrick of sgRNAs contained three parts: a 20-bp sequence complementary to non-template strand of coding sequence region of targeted gene, a 42-bp dCas9 handle, and a 40-bp terminator, which were located under the transcription start site of the promoter $P_{mxaF\text{-}g}$. The *dcas9* derived from *S. pyogenes* was under control of P_{mxaF}, P_{lac}, P_{fumC}, P_{coxB}, or $P_{R/tetO}$. The primer binding sites for inverse PCR are highlighted by yellow (upper panel). **b** Comparison of growth curves and specific growth rate of the recombinant strains of YMZA-1 to 4 carrying the CRISPRi plasmids for interfering with the different regions of *glyA*, in which, the *dcas9* were under control of P_{mxaF}. Data represent means and standard deviations calculated from three biological replicates. Significance was assessed using *t* test, $^{*}p < 0.05$; $^{**}p < 0.01$; $^{***}p < 0.001$

three putative phytoene synthases (META1_1815, META1_1816, META1_3220) (Fig. 6a). We then constructed two CRISPRi libraries, in which Library 1 included 14 sgRNAs interfering with four putative desaturase genes and

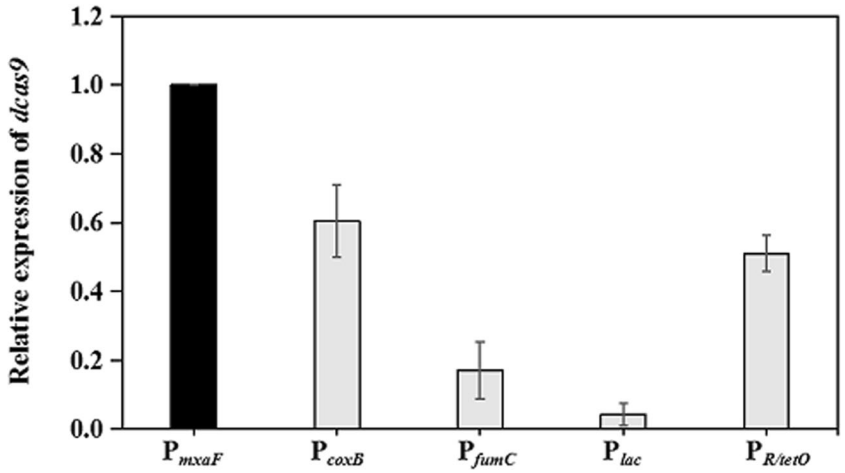

Fig. 2 Comparison of the transcriptional levels acquired by real-time RT-qPCR among the recombinant strains with the CRISPRi plasmids carrying *dcas9* drove by different promoters. For calculating relative expression, the mRNA abundance of *dcas9* was firstly normalized to *rpsB* in each corresponding strain, and then relative expression was the ratio of *dcas9* mRNA between the strains of YMZA-5, YMZA-9, YMZA-13, and YMZA-17 (*dcas9* drove by P_{lac}, P_{fumC}, P_{coxB}, or $P_{R/tetO}$) to the strain YMZA-1 (*dcas9* drove by P_{mxaF}) respectively. Data represent means and standard deviations calculated from three biological replicates

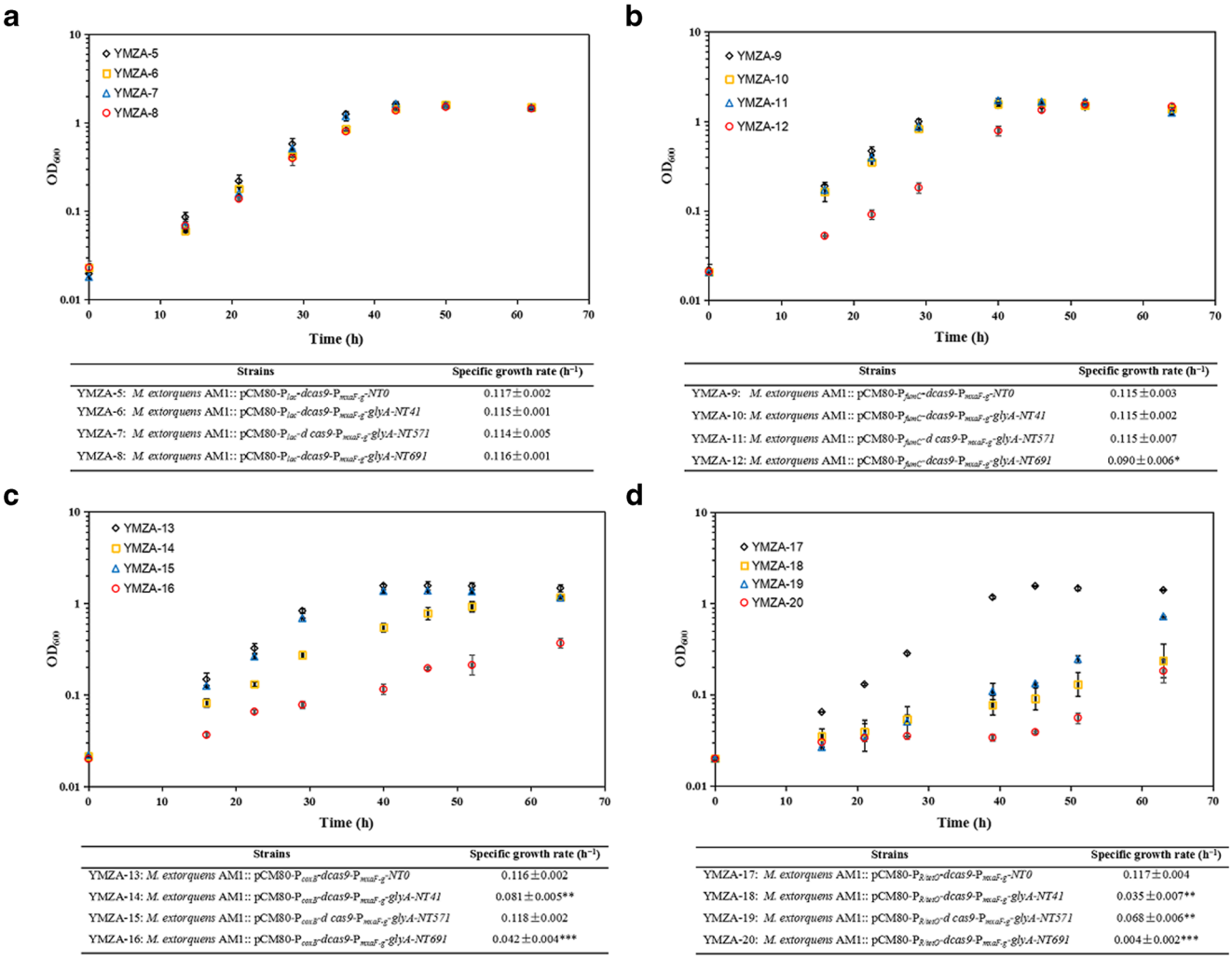

Strains	Specific growth rate (h^{-1})
YMZA-5: *M. extorquens* AM1:: pCM80-P_{lac}-*dcas9*-P_{mxaF-g}-*NT0*	0.117±0.002
YMZA-6: *M. extorquens* AM1:: pCM80-P_{lac}-*dcas9*-P_{mxaF-g}-*glyA-NT41*	0.115±0.001
YMZA-7: *M. extorquens* AM1:: pCM80-P_{lac}-*d cas9*-P_{mxaF-g}-*glyA-NT571*	0.114±0.005
YMZA-8: *M. extorquens* AM1:: pCM80-P_{lac}-*dcas9*-P_{mxaF-g}-*glyA-NT691*	0.116±0.001

Strains	Specific growth rate (h^{-1})
YMZA-9: *M. extorquens* AM1:: pCM80-P_{fumC}-*dcas9*-P_{mxaF-g}-*NT0*	0.115±0.003
YMZA-10: *M. extorquens* AM1:: pCM80-P_{fumC}-*dcas9*-P_{mxaF-g}-*glyA-NT41*	0.115±0.002
YMZA-11: *M. extorquens* AM1:: pCM80-P_{fumC}-*d cas9*-P_{mxaF-g}-*glyA-NT571*	0.115±0.007
YMZA-12: *M. extorquens* AM1:: pCM80-P_{fumC}-*dcas9*-P_{mxaF-g}-*glyA-NT691*	0.090±0.006*

Strains	Specific growth rate (h^{-1})
YMZA-13: *M. extorquens* AM1:: pCM80-P_{coxB}-*dcas9*-P_{mxaF-g}-*NT0*	0.116±0.002
YMZA-14: *M. extorquens* AM1:: pCM80-P_{coxB}-*dcas9*-P_{mxaF-g}-*glyA-NT41*	0.081±0.005**
YMZA-15: *M. extorquens* AM1:: pCM80-P_{coxB}-*d cas9*-P_{mxaF-g}-*glyA-NT571*	0.118±0.002
YMZA-16: *M. extorquens* AM1:: pCM80-P_{coxB}-*dcas9*-P_{mxaF-g}-*glyA-NT691*	0.042±0.004***

Strains	Specific growth rate (h^{-1})
YMZA-17: *M. extorquens* AM1:: pCM80-$P_{R/tetO}$-*dcas9*-P_{mxaF-g}-*NT0*	0.117±0.004
YMZA-18: *M. extorquens* AM1:: pCM80-$P_{R/tetO}$-*dcas9*-P_{mxaF-g}-*glyA-NT41*	0.035±0.007**
YMZA-19: *M. extorquens* AM1:: pCM80-$P_{R/tetO}$-*d cas9*-P_{mxaF-g}-*glyA-NT571*	0.068±0.006**
YMZA-20: *M. extorquens* AM1:: pCM80-$P_{R/tetO}$-*dcas9*-P_{mxaF-g}-*glyA-NT691*	0.004±0.002***

Fig. 3 Optimization of the CRISPRi system in *M. extorquens* AM1. **a**–**d** Comparison of growth curves and specific growth rate of the recombinant strains of YMZA-5 to YMZA-20 carrying the CRISPRi plasmids for interfering with the different regions of *glyA*, in which, the *dcas9* were under control of P_{lac}, P_{fumC}, P_{coxB}, or $P_{R/tetO}$. Data represent means and standard deviations calculated from three biological replicates. Significance was assessed using *t* test, $*p < 0.05$; $**p < 0.01$; $***p < 0.001$

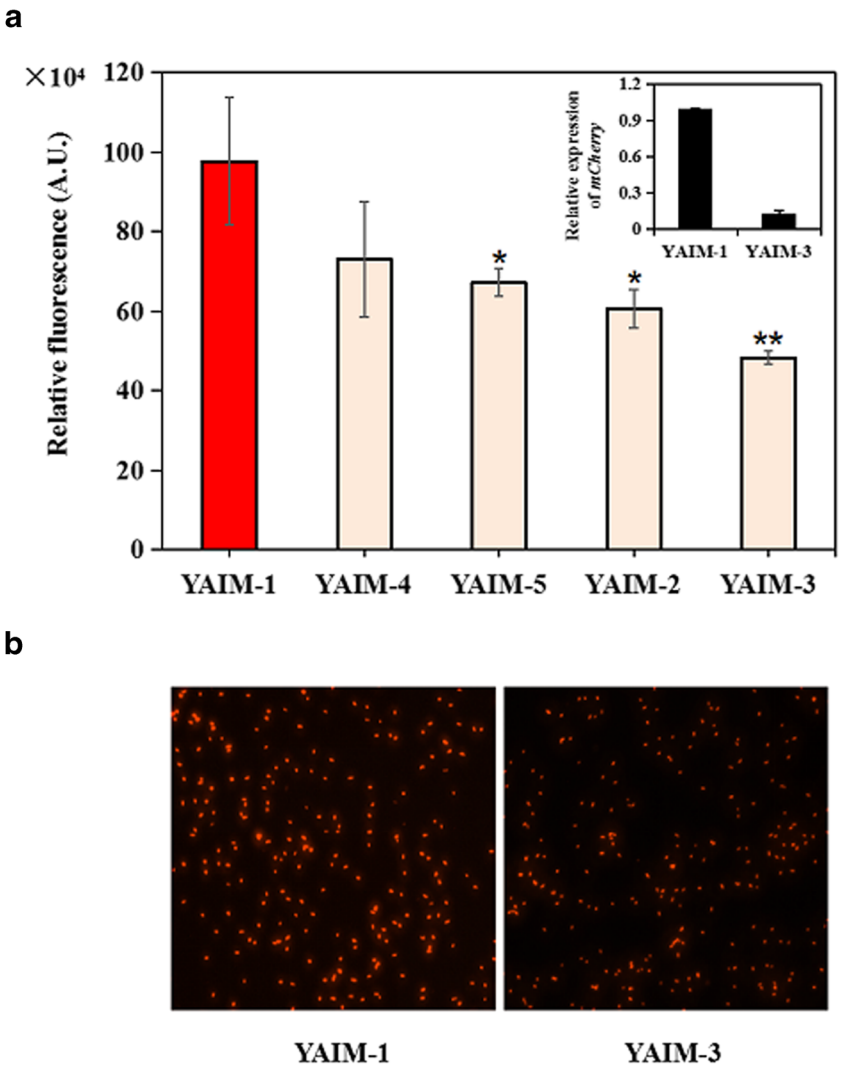

Fig. 4 The repression of *mCherry* by CRISPRi system. The strains of YAIM-2 to 5 carried the sgRNAs targeting different regions of *mCherry* sequence. The inserted panel was the relative expression of *mCherry* between the recombinant strain YAIM-3 and the control strain YAIM-1. The red fluorescence was visualized and quantified by Cytation1 imaging reader. Data represent means and standard deviations calculated from three biological replicates. Significance was assessed using *t* test, $*p < 0.05$; $**p < 0.01$; $***p < 0.001$

crtI (*META1_3665*) and Library 2 included 12 sgRNAs interfering with four putative synthase genes. All 26 sgRNAs were covered by 2470 recombinant strains of *M. extorquens* AM1. For Library 1 with 1320 strains, about 20 to 45% of strains appeared faint pink on each plate as shown an example in Fig. 6c, suggesting that they likely produced less pink carotenoid than that of the wild-type strain. Resultant PCR fragments of sgRNAs from 50 faint pink recombinant strains were re-sequenced, and the distribution of sgRNAs is listed in Table 3. All the sgRNAs from faint pink strains were found to target the gene *META1_3670* encoding putative phytoene desaturase and the control *crtI*. RT-qPCR analysis demonstrated that the mRNA levels of *META1_3670* in the strains of YMZA-24, YMZA-25, and YMZA-26 were reduced by 61.5 to 83.5% (Fig. 6d). Subsequently, to verify the function of *META1_3670*, it was deleted from the chromosome and the mutant strain YAIP was shown colorless on the plate (Fig. 6e). When the mutant strain was complemented with overexpressing *META1_3670*, the complementary strain YACR could restore the pink color and produce about 69% carotenoid of the wild-type strain (Fig. 6 e and f; Fig. S3A). All these results clearly demonstrated the gene *META1_3670* was involved in the carotenoid biosynthetic pathway in *M. extorquens* AM1. Moreover, phylogenetic analysis revealed that the sequences of phytoene desaturase respectively encoded by *crtI* (*META1_3665*) and *META1_3670* were diverged from each other (Fig. S4). *META1_3670* encoding a desaturase and its homologous proteins from other species of *Methylobacteria* indicated a close evolutionary relationship to ζ-carotene desaturase CrtQa from *Nostoc* sp. PCC 7120 and CrtIb from *Myxococcus xanthus* (Fig. S4). CrtQa has been demonstrated to possess the function of *Z* to *E* isomerase and CrtIb has been validated to dehydrogenate carotenes in the *trans*-conformation (Breitenbach et al. 2013; Iniesta et al. 2007; Botella et al. 1995). Thus, we hypothesized that the enzymes encoded by *META1_3670* and *crtI* might be responsible for dehydrogenating carotenes with different conformation and that cooperation of two carotene desaturases could result in

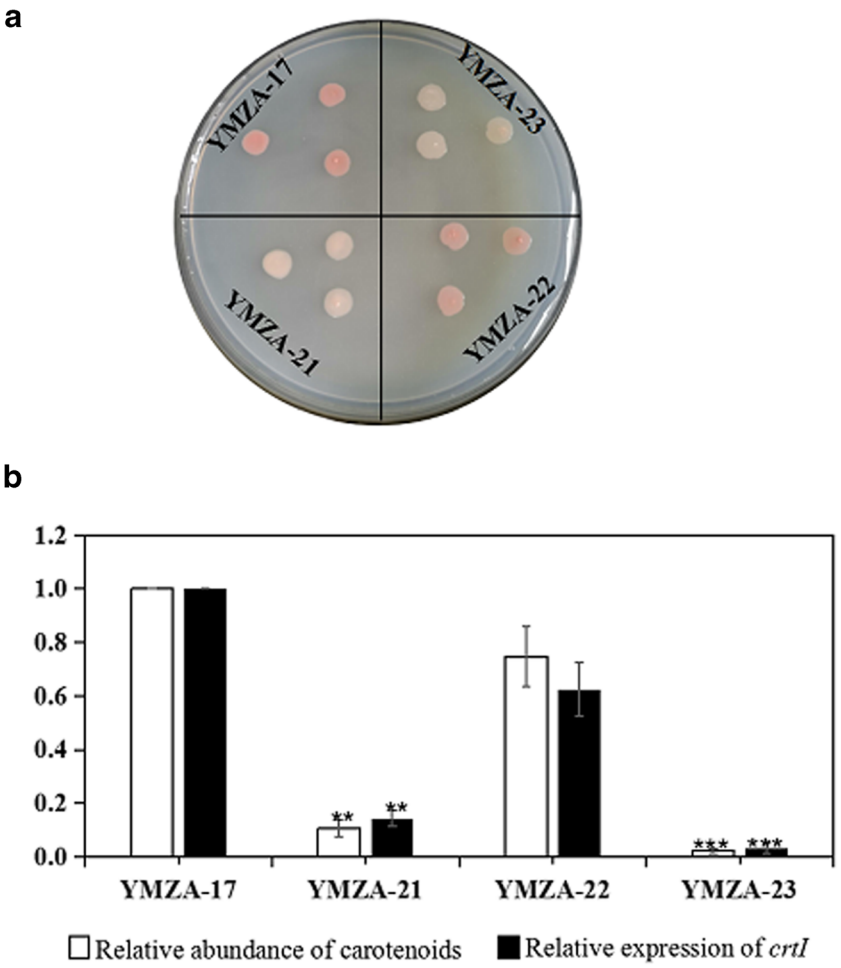

Fig. 5 The repression of *crtI* by CRISPRi system. **a** Comparison of the change of colony color among the recombinant strains carrying different CRISPRi plasmids. **b** The relative expression of *crtI* and production of carotenoids between the recombinant strains (YMZA-21, YMZA-22, and YMZA-23) and the control strain YMZA-17. RT-qPCR analysis and production measurement are performed in three biological replicates. Significance was assessed using *t* test, $*p < 0.05$; $**p < 0.01$; $***p < 0.001$

completing the four dehydrogenation steps in *M. extorquens* AM1.

However, for Library 2 with 1150 strains, 12 sgRNAs targeting three predicted synthase genes did not result in any change of colony color on the plate (Fig. S5A). We then knocked out the previously annotated *crtB* (*META1_3220*) and did not observe the changed color of colonies either in the mutant strain of YAIB (Fig. S3B and Fig. S5B). Our current results proposed that other unknown genes are likely responsible for this reaction. It also did not rule out the redundant function of these three predicted genes, meaning that single gene knockdown or deletion was not enough to significantly change the cell phenotype.

Application of CRISPRi to enhance the production of carotenoid by knocking down a competitive pathway

In recent years, *M. extorquens* has attracted the attention to be developed as a single cell protein for aquaculture (Tlusty et al. 2017). One particular beneficial trait is that *M. extorquens* produces a suite of natural carotenoid pigments that have been associated with both imparting color and enhancing immunity of shrimps and fishes (Tlusty et al. 2017). In order to improve the production of carotenoid, one plausible strategy is to increase the supply of precursor intermediates. In *M. extorquens* AM1, the biosynthesis of carotenoid and hopanoid shares the same precursor isoprene. And the squalene-hopene cyclase encoded by gene *shc* is an essential enzyme for the hopanoid

Fig. 6 Mining the putative enzymes involved in carotenoid biosynthesis by CRISPRi with pooled sgRNAs. **a** The putative phytoene synthases in orange and phytoene desaturases in red participating in carotenoid synthesis. **b** The schematic chart for interference of putative phytoene synthases and desaturases. **c** The color of colonies was changed due to the repression of putative phytoene desaturases. **d** The relative expression of phytoene desaturase gene *META1_3670* in the recombinant strains carrying different CRISPRi plasmids. **e** Functional analysis of *META1_3670* by deletion and gene complementation. **f** Comparison of carotenoid production in the recombinant strains. The YMZA-17 strain carried the plasmid with the control sgRNA, and the strains of YMZA-24 to YMZA-26 carried the plasmids targeting different regions of the non-template strand of *META1_3670*. YAIP was the strain with deleted *META1_3670*. YACR was the strain with *META1_3670* reintroduced into the YAIP strain. RT-qPCR analysis and production measurement are performed in three biological replicates. Significance was assessed using *t* test, $*p < 0.05$; $**p < 0.01$; $***p < 0.001$

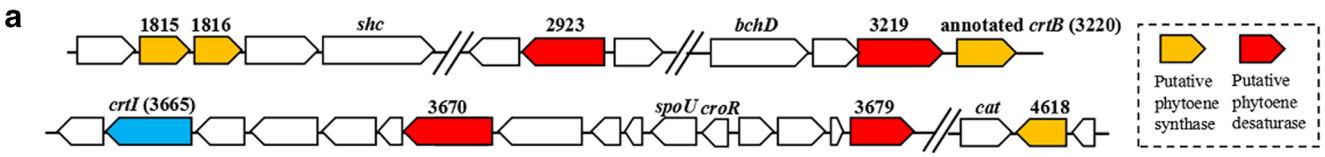
a
1815 1816
shc
2923
bchD
3219
annotated crtB (3220)
crtI (3665)
3670
spoU croR
3679
cat
4618
Putative phytoene synthase
Putative phytoene desaturase

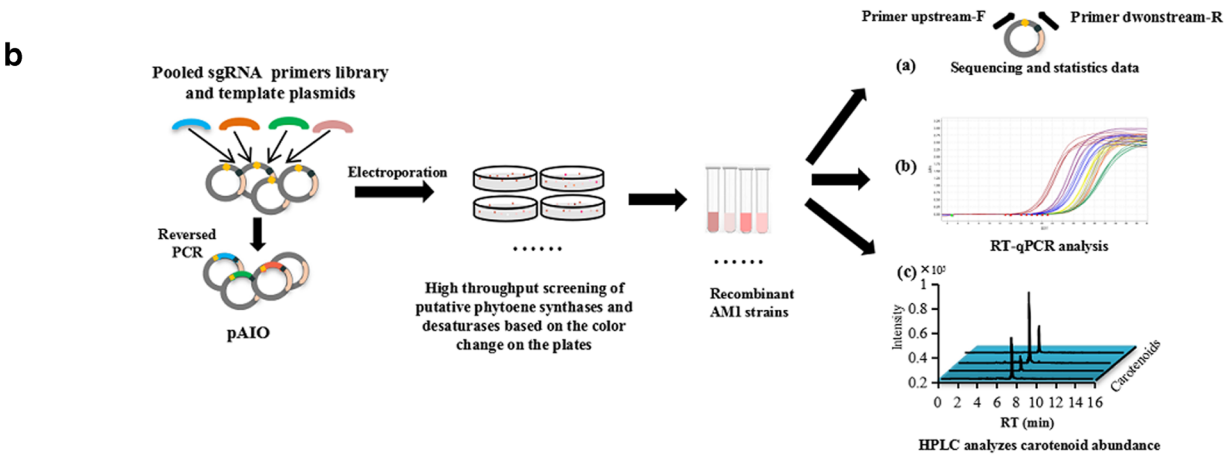
b
Pooled sgRNA primers library and template plasmids
Electroporation
Reversed PCR
pAIO
High throughput screening of putative phytoene synthases and desaturases based on the color change on the plates
Recombinant AM1 strains
Primer upstream-F
Primer dwonstream-R
(a)
Sequencing and statistics data
(b)
RT-qPCR analysis
(c)
Intensity
Carotenoids
RT (min)
HPLC analyzes carotenoid abundance

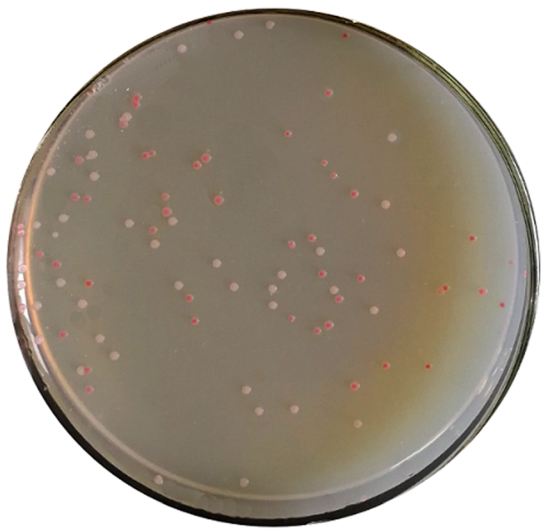
c

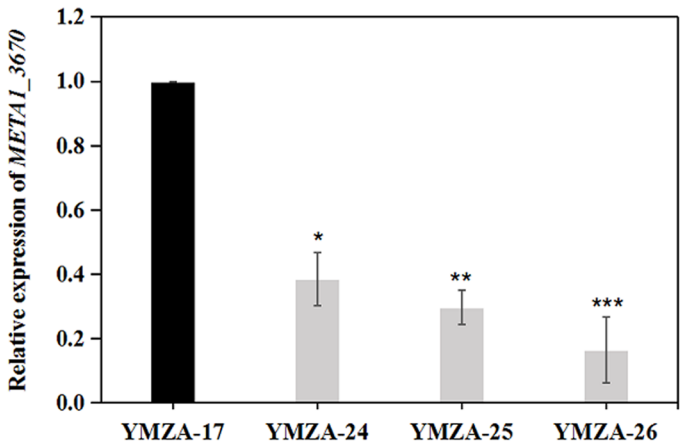
d
Relative expression of METAL_3670
1.2
1.0
0.8
0.6
0.4
0.2
0.0
*
**
***
YMZA-17
YMZA-24
YMZA-25
YMZA-26

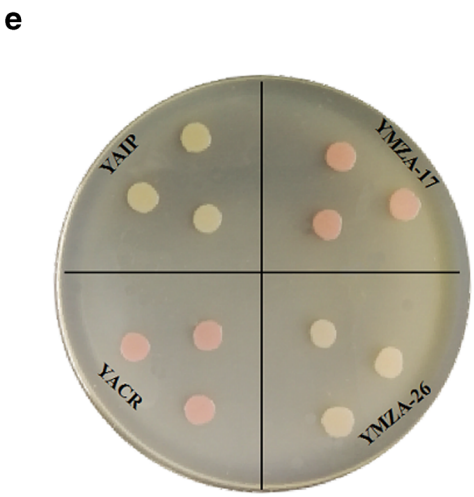
e
YAIP
YMZA-17
YACR
YMZA-26

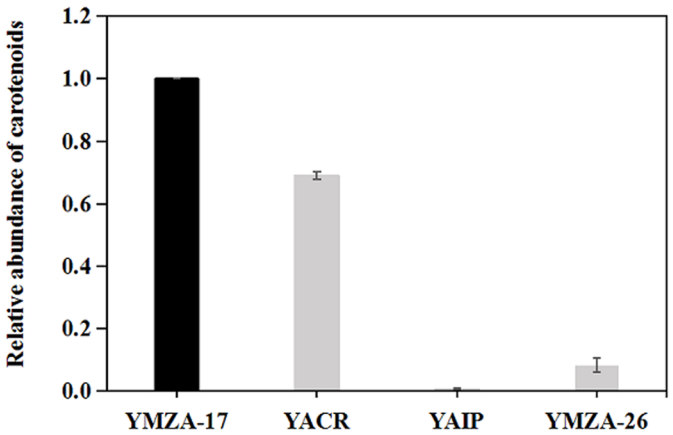
f
Relative abundance of carotenoids
1.2
1.0
0.8
0.6
0.4
0.2
0.0
YMZA-17
YACR
YAIP
YMZA-26

biosynthesis (Bradley et al. 2017). Because the hopanoid is important for membrane fluidity and lipid packing, the direct deletion of *shc* can cause the mutant strain to alter physiological properties and suppress growth (Bradley et al. 2017; Sáenz et al. 2015). Here, we evaluated whether we could enhance the production of carotenoid by knocking down the expression of *shc* through CRISPRi without disturbing the growth phenotype. Three CRISPRi plasmids were constructed to target different sites of *shc*. By comparison of the control strain YMZA-17, the production of carotenoid was not significantly improved in the strains of YMZA-27 and YMZA-28 but was increased by 1.9-fold in the recombinant strain YMZA-29 (Fig. 7a). Meanwhile, the growth rate and biomass yield of the strain YMZA-29 did not change significantly (Fig. 7b; Table S2). RT-qPCR analysis demonstrated that the mRNA levels of *shc* in the strains YMZA-27 to YMZA-29 dropped to 42.2%, 75.7%, and 35.1% of that of the wild-type strain, respectively (Fig. 7a). Therefore, with designing the sgRNAs targeting different sites, the developed CRISPRi could be applied to enhance the production of targeted metabolites through downregulating the expression of genes involved in the competitive pathway with the essential function in physiological process.

Discussion

M. extorquens AM1 is capable of growing on C1 compounds as the sole carbon and energy source, which makes it a promising cell factory for biotechnology in a methanol- and formate-based bioeconomy. Its central carbon metabolism pathways such as the serine cycle and EMC pathway contain C2 to C5 intermediates that are all interesting precursors for producing value-added chemicals such as mevalonate, 3-hydroxypropionate, and 1-butanol (Schada et al. 2018). Thus, the relevant genes in these pathways cannot be simply deleted for pushing the flux through the certain intermediate because the knockouts usually result in a lethal growth phenotype on C1 compounds. In view of this, CRISPRi provides a useful tool to fine-tune transcriptional level of essential genes and channel flux through biosynthetic pathways of targeted products. In this study, a CRISPRi system was developed to effectively knock down the gene expression in *M. extorquens* AM1. The highest interference efficacy was found to be *dcas9* under control of $P_{R/tetO}$ without the TetR repressor and sgRNA under control of strong promoter $P_{mxaF\text{-}g}$. In general, the highest repression efficacy can be achieved in which both *dcas9* and sgRNA were droved by strong promoters (Fontana et al. 2018); however, for *M. extorquens* AM1, no significant repression efficacy was achieved when both *dcas9* and sgRNA were droved by strong P_{mxaF}. We propose that an appropriate balance of expression level of *dcas9* and sgRNA was critically important to determine the efficiency of CRISPRi in *M. extorquens* AM1. Similar phenomena have also been observed in other bacteria such as *E. coli*, in which expression of *dcas9* by a moderate level promoter and the sgRNA by strong promoter achieved the optimal production of isopentenol (Tian et al. 2019). Inducible promoters are often applied to control the dynamic expression of *dcas9* to achieve dynamic repression of target gene with different concentrations of inducers (Wang et al. 2019; Tan et al. 2018). In *M. extorquens* AM1, the inducible promoters confer weak or leaky expression under control of repressor (Marx and Lidstrom 2001), and in this study, we tried to use inducible promoter $P_{R/tetO}$ along with its repressor TetR to dynamically regulate the repression of gene expression, whereas it did not make the improvement of repression efficacy.

Previous studies have demonstrated that variant sgRNAs targeting different regions show important relationship with repression efficacy, which was also observed in our study by the repression activity of *glyA*, *mCherry*, *crtI*, *META1_3670*, and *shc*. When sgRNA targeting the beginning region of the transcript or − 10 and − 35 regions of promoter, it is indicated to result in higher repression (Larson et al. 2013; Qi et al. 2013; Du et al. 2017; Huang et al. 2016). However, for interfering the coding region, it is difficult to accurately predict which locus region on the non-template strand would be more suitable for achieving high interference efficacy. Many reports have revealed that the sgRNA targeting the coding region of non-template strand with small distance to transcriptional start site can achieve better repression efficacy (Zhan et al. 2019; Li et al. 2017; Hogan et al. 2019), but sometimes, the repression efficacy of sgRNA is not well correlated to the distance (Tao et al. 2017; McInally et al. 2019). For *M. extorquens* AM1, as shown from the repression efficacy interfering *glyA*, *crtI*, *META1_3670*, and *shc*, it was more likely that interfering initial and terminal coding region of non-template strands both showed good repression efficacy. By this developed CRISPRi technology, we successfully knocked down the transcriptional level of squalene-hopene cyclase gene *shc* without influencing cell growth and introduced more flux into carotene biosynthesis resulting in an about 2-fold improvement in carotenoid production.

Table 3 Proportion of 50 sgRNAs sequenced from faint pink strains generated by interference of four putative phytoene desaturases gene and one identified phytoene desaturase *crtI* by using CRISPRi

Targeted sites of sgRNAs	Proportion of sgRNAs (%)
META1_3665-NT6	9.62
META1_3665-NT1168	5.77
META1_3670-NT29	23.08
META1_3670-NT815	44.23
META1_3670-NT1500	17.30

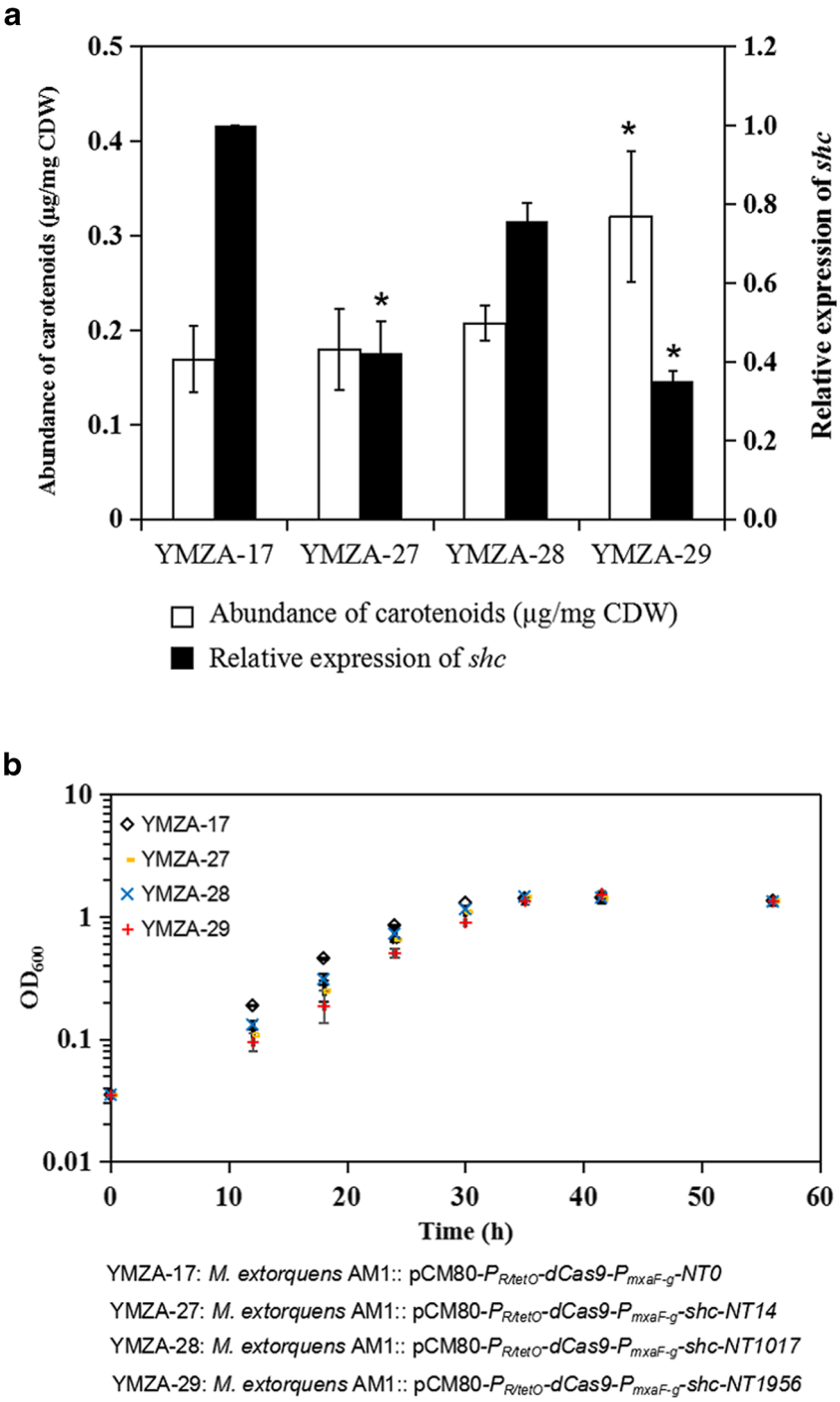

Fig. 7 Improvement of the carotenoid production in *M. extorquens* AM1 through interfering the expression of *shc*. **a** The relative expression of *shc* and relative production of carotenoid in the recombinant strains. **b** Comparison of growth curve of the recombinant strains. RT-qPCR analysis, production measurement, and growth analysis are performed in three biological replicates. Significance was assessed using *t* test, $*p < 0.05$; $**p < 0.01$; $***p < 0.001$

CRISPRi has been demonstrated to be very useful in identifying targeted gene from a series of candidate genes in traditional industrial strains such as *E. coli* and *Corynebacterium glutamicum* and in the human pathogen *Vibrio cholerae* (Wang et al. 2018; Lee et al., 2018; Caro et al. 2019). For instance, by using CRISPRi technology, Lee et al. rapidly identify an unknown carboxyl esterase for degradation of methyl acetate in *C. glutamicum* (Lee et al., 2018). In this study, by application of the CRISPRi system with a small pool of sgRNAs, we rapidly screened out a new phytoene desaturase encoded by *META1_3670* responsible for carotenoid biosynthesis. Whereas Van Dien et al. identified a phytoene desaturase CrtI (META1_3665) participating in carotenoid biosynthesis from approximately 7000 screened visually through transposon mutagenesis technology (Van Dien et al. 2003), CRISPRi developed here presented to be a high throughput genetic tool to achieve precise interference of a number of candidate genes and reduce insertion bias on the

chromosome. Up to now, many bacterial carotenoid biosynthetic genes are reported to form a cluster pattern (Tian and Hua 2010), and only a few characterized examples, such as in *Gemmatimonas aurantiaca*, *Deinococcus radiodurans*, and *Salinispora tropica*, have been found to either be not colocalized or be loosely clustered and, thus, not co-transcribed (Tian and Hua 2010; Takaichi et al. 2010; Richter et al. 2015). Moreover, one single phytoene desaturase has been demonstrated to be enough to catalyze four desaturation steps to produce lycopene in bacteria (Tian and Hua 2010; Fischbach and Voigt 2010; Paniagua et al. 2012). So far, there is only one example found in *Myxococcus xanthus* that two carotenoid desaturases CrtIa and CrtIb are required to complete four desaturation steps to convert phytoene into lycopene (Iniesta et al. 2007). In addition, in cyanobacteria and plants, phytoene desaturase Pds and ζ-carotene desaturase Zds have been also described to catalyze the sequential conversion from phytoene to ζ-carotene, and then, to lycopene (Nupur et al. 2016; Hirschberg 2001; Nisar et al. 2015). Our study provides the second example in bacteria that two desaturases encoding by *META1_3665* and *META1_3670* are involved in carotenoid biosynthesis. For the chemical structures of carotenoids in methylotrophic bacteria, currently, it has not been well demonstrated except for a few species (Sato et al. 1982; Ayako et al. 2015). For instance, four carotenoids with an attached sugar moiety have been isolated from six *Methylobacterium* strains (i.e., *Methylobacterium* sp. 189, *Methylobacterium* sp. 32, *Methylobacterium* sp. F15, *Methylobacterium* sp. 680, *M. populi* BJ00118 and *M. radiotolerans* JCM2831) (Ayako et al. 2015). The structures of carotenoids produced by *M. extorquens* AM1 were proposed to be similar with that produced by *Methylobacterium* strains (Ayako et al.2015) according to their accurate mass and UV absorption (data not shown), which could be the C30-carotenoids with a β-glucose and a fatty acid chain. Considering the exact structures of carotenoids in *M. extorquens* AM1 are still unclear at this moment, it is difficult to postulate the clear role that each desaturase played. The characterization of the chemical structures and enzymatic function are subjects of ongoing research.

A number of genes are poorly identified in the model methylotroph of *M. extorquens* AM1, leading to a large challenge of engineering this type of bacterium as a powerful chassis host. Our work herein demonstrates that the developed CRISPRi system can efficiently and gradually repress the expression of diverse targeted genes in *M. extorquens* AM1, providing an important basis for further uncovering unknown gene functions with pooled sgRNA libraries in a high-throughput phenotypic screening approach. Additionally, fine-tuning gene expression by CRISPRi provides a valuable strategy for gene knockdown of competing pathways to channel more flux into the desired pathway.

Acknowledgments We thank Joseph D. Groom and Mary E. Lidstrom at the University of Washington for their assistance with English editing.

Author contributions HZ and XM perform the experiments. SY and XM conceived the experiments, SY, XM, TW, CZ, CZ, and XX analyzed data. XM and SY wrote the manuscript. All authors read and approved the manuscript.

Funding information This work was supported by the National Key R&D Program of China (grant No. 2018YFA0901500); the National Natural Science Foundation of China (grant No. 21776149); Shandong Provincial Key Research and Development Project, China (2016GSF117026); and Shandong Provincial Natural Science Foundation, China (ZR2015CM017).

Compliance with ethical standards

This article does not contain any studies with human participants or animals performed by any of the authors.

Conflict of interest The authors declare that they have no conflict of interest.

References

Ayako O, Kaseya Y, Koue N, Schrader J, Knief C, Vorholt JA, Sandmann G, Shindo K (2015) 4-[2-O-11Z-Octadecenoyl-β-glucopyranosyl]-4,4′-diapolycopene-4,4′-dioic acid and 4-[2-O-9Z-hexadecenoyl-β-glucopyranosyl]-4,4′-diapolycopene-4,4′-dioic acid: new C30-carotenoids produced by *Methylobacterium*. Tetrahedron Lett 56: 2791–2794. https://doi.org/10.1016/j.tetlet.2015.04.042

Botella JA, Murillo FJ, Ruiz-Vázquez R (1995) A cluster of structural and regulatory genes for light-induced carotenogenesis in *Myxococcus xanthus*. Eur J Biochem 233:238–248. https://doi.org/10.1111/j.1432-1033.1995.238_1.x

Bradley AS, Swanson PK, Muller EE, Bringel F, Caroll SM, Pearson A, Vuilleumier S, Marx CJ (2017) Hopanoid-free *Methylobacterium extorquens* DM4 overproduces carotenoids and has widespread growth impairment. PLoS One 12:e0173323. https://doi.org/10.1371/journal.pone.0173323

Breitenbach J, Bruns M, Sandmann G (2013) Contribution of two ζ-carotene desaturases to the poly-cis desaturation pathway in the cyanobacterium *Nostoc* PCC 7120. Arch Microbiol 195:491–498. https://doi.org/10.1007/s00203-013-0899-1

Bruder MR, Pyne ME, Moo-Young M, Chung DA, Chou CP (2016) Extending CRISPR-Cas9 technology from genome editing to transcriptional engineering in the genus *Clostridium*. Appl Environ Microbiol 82:6109–6119. https://doi.org/10.1128/AEM.02128-16

Caro F, Place NM, Mekalanos JJ (2019) Analysis of lipoprotein transport depletion in *Vibrio cholerae* using CRISPRi. Proc Natl Acad Sci U S A 116:17013–17022. https://doi.org/10.1073/pnas.1906158116

Chou HH, Marx CJ (2012) Optimization of gene expression through divergent mutational paths. Cell Rep 1:133–140. https://doi.org/10.1016/j.celrep.2011.12.003

Chou HH, Berthet J, Marx CJ (2009) Fast growth increases the selective advantage of a mutation arising recurrently during evolution under metal limitation. PLoS Genet 5:e1000652. https://doi.org/10.1371/journal.pgen.1000652

Choudhary E, Thakur P, Pareek M, Agarwal N (2015) Gene silencing by CRISPR interference in mycobacteria. Nat Commun 6:6267. https://doi.org/10.1038/ncomms7267

Chubiz LM, Purswani J, Carroll SM, Marx CJ (2013) A novel pair of inducible expression vectors for use in *Methylobacterium*

extorquens. BMC Res Notes 6:183. https://doi.org/10.1186/1756-0500-6-183

Cleto S, Jensen JV, Wendisch VF, Lu TK (2016) *Corynebacterium glutamicum* metabolic engineering with CRISPR interference (CRISPRi). ACS Synth Biol 5:375–385. https://doi.org/10.1021/acssynbio.5b00216

Du D, Roguev A, Gordon DE, Chen M, Chen SH, Shales M, Shen JP, Ideker T, Mali P, Qi LS, Krogan NJ (2017) Genetic interaction mapping in mammalian cells using CRISPR interference. Nat Methods 14(6):577–580. https://doi.org/10.1038/nmeth.4286

Fischbach M, Voigt CA (2010) Prokaryotic gene clusters: a rich toolbox for synthetic biology. Biotechnol J 5:1277–1296. https://doi.org/10.1002/biot.201000181

Fontana J, Dong C, Ham JY, Zalatan JG, Carothers JM (2018) Regulated Expression of sgRNAs Tunes CRISPRi in *E. coli*. J Bacteriol. 13(9): e1800069. https://doi.org/10.1002/biot.201800069

Fukaya Y, Takemura M, Koyanagi T, Maoka T, Shindo K, Misawa N (2018) Structural and functional analysis of the carotenoid biosynthesis genes of a *Pseudomonas* strain isolated from the excrement of autumn darter. Biosci Biotechnol Biochem 82:1043–1052. https://doi.org/10.1080/09168451.2017.1398069

Gilbert LA, Horlbeck MA, Adamson B, Villalta JE, Chen Y, Whitehead EH, Guimaraes C, Panning B, Ploegh HL, Bassik MC, Qi LS, Kampmann M, Weissman JS (2014) Genome-scale CRISPR-mediated control of gene repression and activation. Cell 159:647–661. https://doi.org/10.1016/j.cell.2014.09.029

Guo J, Wang T, Guan C, Liu B, Luo C, Xie Z, Zhang C, Xing XH (2018) Improved sgRNA design in bacteria via genome-wide activity profiling. Nucleic Acids Res 46:7052–7069. https://doi.org/10.1093/nar/gky572

Harcombe WR, Betts A, Shapiro JW, Marx CJ (2016) Adding biotic complexity alters the metabolic benefits of mutualism. Evolution 70(8):1871–1881. https://doi.org/10.1111/evo.12973

Hirschberg J (2001) Carotenoid biosynthesis in flowering plants. Curr Opin Plant Biol 4:210–218. https://doi.org/10.1016/S1369-5266(00)00163-1

Hogan AM, Rahman ASMZ, Lightly TJ, Cardona ST (2019) A broad-host-range CRISPRi toolkit for silencing gene expression in *Burkholderia*. ACS Synth Biol 8:2372–2384. https://doi.org/10.1021/acssynbio.9b00232

Hu B, Yang YM, Beck DA, Wang QW, Chen WJ, Yang J, Lidstrom ME, Yang S (2016) Comprehensive molecular characterization of *Methylobacterium extorquens* AM1 adapted for 1-butanol tolerance. Biotechnol Biofuels 9:84. https://doi.org/10.1186/s13068-016-0497-y

Huang CH, Shen CR, Li H, Sung LY, Wu MY, Hu YC (2016) CRISPR interference (CRISPRi) for gene regulation and succinate production in cyanobacterium *S. elongatus* PCC 7942. Microb Cell Factories 15:196. https://doi.org/10.1186/s12934-016-0595-3

Iniesta AA, Cervantes M, Murillo FJ (2007) Cooperation of two carotene desaturases in the production of lycopene in *Myxococcus xanthus*. FEBS J 274:4306–4314. https://doi.org/10.1111/j.1742-4658.2007.05960.x

Larson MH, Gilbert LA, Wang X, Lim WA, Weissman JS, Qi LS (2013) CRISPR interference (CRISPRi) for sequence-specific control of gene expression. Nat Protoc 8:2180–2196. https://doi.org/10.1038/nprot.2013.132

Lee SS, Shin H, Jo S, Lee SM, Um Y, Woo HM (2018) Rapid identification of unknown carboxyl esterase activity in *Corynebacterium glutamicum* using RNA-guided CRISPR interference. Enzym Microb Technol 114:63–68. https://doi.org/10.1016/j.enzmictec.2018.04.004

Lee HH, Ostrov N, Wong BG, Gold MA, Khalil AS, Church GM (2019) Functional genomics of the rapidly replicating bacterium *Vibrio natriegens* by CRISPRi. Nat Microbiol 4:1105–1113. https://doi.org/10.1038/s41564-019-0423-8

Li D, Lv L, Chen JC, Chen GQ (2017) Controlling microbial PHB synthesis via CRISPRi. Appl Microbiol Biotechnol 101:5861–5867. https://doi.org/10.1007/s00253-017-8374-6

Liang WF, Cui LY, Cui JY, Yu KW, Yang S, Wang TM, Guan CG, Zhang C, Xing XH (2017) Biosensor-assisted transcriptional regulator engineering for *Methylobacterium extorquens* AM1 to improve mevalonate. Metab Eng 39:159–168. https://doi.org/10.1016/j.ymben.2016.11.010

Lv L, Ren YL, Chen JC, Wu Q, Chen GQ (2015) Application of CRISPRi for prokaryotic metabolic engineering involving multiple genes, a case study: controllable P(3HB-co-4HB) biosynthesis. Metab Eng 29:160–168. https://doi.org/10.1016/j.ymben.2015.03.013

Marx CJ (2008) Development of a broad-host-range sacB-based vector for unmarked allelic exchange. BMC Res Notes 1:1. https://doi.org/10.1186/1756-0500-1-1

Marx CJ, Lidstrom ME (2001) Development of improved versatile broad-host-range vectors for use in methylotrophs and other gram-negative bacteria. Microbiology 147:2065–2075. https://doi.org/10.1099/00221287-147-8-2065

McInally SG, Hagen KD, Nosala C, Williams J, Nguyen K, Booker J, Jones K, Dawson SC (2019) Robust and stable transcriptional repression in *Giardia* using CRISPRi. Mol Biol Cell 30:119–130. https://doi.org/10.1091/mbc.E18-09-0605

Nayak DD, Agashe D, Lee MC, Marx CJ (2016) Selection maintains apparently degenerate metabolic pathways due to tradeoffs in using methylamine for carbon versus nitrogen. Curr Biol 26:1416–1426. https://doi.org/10.1016/j.cub.2016.04.029

Nisar N, Li L, Lu S, Khin NC, Pogson BJ (2015) Carotenoid metabolism in plants. Mol Plant 8:68–82. https://doi.org/10.1016/j.molp.2014.12.007

Nunn DN, Lidstrom ME (1986) Phenotypic characterization of 10 methanol oxidation mutant classes in *Methylobacterium* sp. strain AM1. J Bacteriol 166(2):591–597. https://doi.org/10.1128/jb.166.2.591-597.1986

Nupur LN, Vats A, Dhanda SK, Raghava GP, Pinnaka AK, Kumar A (2016) ProCarDB: a database of bacterial carotenoids. BMC Microbiol 16:96–98. https://doi.org/10.1186/s12866-016-0715-6

Ochsner AM, Christen M, Hemmerle L, Peyraud R, Christen B, Vorholt JA (2017) Transposon sequencing uncovers an essential regulatory function of phosphoribulokinase for methylotrophy. Curr Biol 27:2579–2588. https://doi.org/10.1016/j.cub.2017.07.025

Paniagua-Michel J, Olmos-Soto J, Ruiz MA (2012) Pathways of carotenoid biosynthesis in bacteria and microalgae. Methods Mol Biol 892:1–12. https://doi.org/10.1007/978-1-61779-879-5_1

Park J, Shin H, Lee SM, Um Y, Woo HM (2018) RNA-guided single/double gene repressions in *Corynebacterium glutamicum* using an efficient CRISPR interference and its application to industrial strain. Microb Cell Factories 17:4. https://doi.org/10.1186/s12934-017-0843-1

Peel D, Quayle JR (1961) Microbial growth on C1 compounds. 1. Isolation and characterization of *Pseudomonas* AM1. Biochem J 81:465–469. https://doi.org/10.1042/bj0810465

Qi LS, Larson MH, Gilbert LA, Doudna JA, Weissman JS, Arkin AP, Lim WA (2013) Repurposing CRISPR as an RNA-guided platform for sequence-specific control of gene expression. Cell 152:1173–1183. https://doi.org/10.1016/j.cell.2013.02.022

Richter TK, Hughes CC, Moore BS (2015) Sioxanthin, a novel glycosylated carotenoid, reveals an unusual subclustered biosynthetic pathway. Environ Microbiol 17:2158–2171. https://doi.org/10.1111/1462-2920.12669

Rohde MT, Tischer S, Harms H, Rohwerder T (2017) Production of 2-hydroxyisobutyric acid from methanol by *Methylobacterium extorquens* AM1 expressing (R)-3-hydroxybutyryl coenzyme a-isomerizing enzymes. Appl Environ Microbiol 83:e02622–e02616. https://doi.org/10.1128/AEM.02622-16

Sáenz JP, Grosser D, Bradley AS, Lagny TJ, Lavrynenko O, Broda M, Simons K (2015) Hopanoids as functional analogues of cholesterol in bacterial membranes. Proc Natl Acad Sci U S A 112(38):11971–11976. https://doi.org/10.1073/pnas.1515607112

Sato K, Mizutani T, Hiraoka M, Shimizu S (1982) Carotenoid containing sugar moiety from a facultative methylotroph, *Protaminobacter ruber*. J Ferment Technol 60:111–115

Schada von Borzyskowski L, Remus-Emsermann M, Weishaupt R, Vorholt JA, Erb TJ (2015) A set of versatile brick vectors and promoters for the assembly, expression, and integration of synthetic operons in *Methylobacterium extorquens* AM1 and other alphaproteobacteria. ACS Synth Biol 4:430–443. https://doi.org/10.1021/sb500221v

Schada von Borzyskowski L, Sonntag F, Pöschel L, Vorholt JA, Schrader J, Erb TJ1, Buchhaupt M (2018) Replacing the ethylmalonyl-CoA pathway with the glyoxylate shunt provides metabolic flexibility in the central carbon metabolism of *Methylobacterium extorquens* AM1. ACS Synth Biol 7:86–97. https://doi.org/10.1021/acssynbio.7b00229

Schultenkämper K, Brito LF, López MG, Brautaset T, Wendisch VF (2019) Establishment and application of CRISPR interference to affect sporulation, hydrogen peroxide detoxification, and mannitol catabolism in the methylotrophic thermophile *Bacillus methanolicus*. Appl Microbiol Biotechnol 103:5879–5889. https://doi.org/10.1007/s00253-019-09907-8

Sedkova N, Tao L, Rouvière PE, Cheng Q (2005) Diversity of carotenoid synthesis gene clusters from environmental *Enterobacteriaceae* strains. Appl Environ Microbiol 71:8141–8146. https://doi.org/10.1128/AEM.71.12.8141-8146.2005

Smejkalová H, Erb TJ, Fuchs G (2010) Methanol assimilation in *Methylobacterium extorquens* AM1: demonstration of all enzymes and their regulation. PLoS One 5:e13001. https://doi.org/10.1371/journal.pone.0013001

Takaichi S, Maoka T, Takasaki K, Hanada S (2010) Carotenoids of *Gemmatimonas aurantiaca* (*Gemmatimonadetes*): identification of a novel carotenoid, deoxyoscillol 2-rhamnoside, and proposed biosynthetic pathway of oscillol 2,2′-dirhamnoside. Microbiology 156:757–763. https://doi.org/10.1099/mic.0.034249-0

Tan SZ, Reisch CR, Prather KLJ (2018) A robust CRISPR interference gene repression system in *Pseudomonas*. J Bacteriol 200:e00575–17. https://doi.org/10.1128/JB.00575-17

Tao W, Lv L, Chen GQ (2017) Engineering *Halomonas* species TD01 for enhanced polyhydroxyalkanoates synthesis via CRISPRi. Microb Cell Factories 16:48. https://doi.org/10.1186/s12934-017-0655-3

Tapscott T, Guarnieri MT, Henard CA (2019) Development of a CRISPR/Cas9 system for *Methylococcus capsulatus* in vivo gene editing. Appl environ Microbiol 85. Pii: e00340-e00319. doi: https://doi.org/10.1128/AEM.00340-19

Tian B, Hua Y (2010) Carotenoid biosynthesis in extremophilic Deinococcus-Thermus bacteria. Trends Microbiol 18:512–520. https://doi.org/10.1016/j.tim.2010.07.007

Tian T, Kang JW, Kang A, Lee TS (2019) Redirecting metabolic flux via combinatorial multiplex CRISPRi-mediated repression for isopentenol production in *Escherichia coli*. ACS Synth Biol 8:391–402. https://doi.org/10.1021/acssynbio.8b00429

Tlusty M, Rhyne A, Szczebak JT, Bourque B, Bowen JL, Burr G, Marx CJ, Feinberg L (2017) A transdisciplinary approach to the initial validation of a single cell protein as an alternative protein source for use in aquafeeds. Peer J 5:e3170. https://doi.org/10.7717/peerj.3170

Ueoka R, Bortfeld-Miller M, Morinaka BI, Vorholt JA, Piel J (2018) Toblerols: cyclopropanol-containing polyketide modulators of antibiosis in *Methylobacteria*. Angew Chem Int Ed 57:977–981. https://doi.org/10.1002/anie.201709056

Van Dien SJ, Marx CJ, O'Brien BN, Lidstrom ME (2003) Genetic characterization of the carotenoid biosynthetic pathway in *Methylobacterium extorquens* AM1 and isolation of a colorless mutant. Appl Environ Microbiol 69:7563–7566. https://doi.org/10.1128/AEM.69.12.7563-7566.2003

Vuilleumier S, Chistoserdova L, Lee MC, Bringel F, Lajus A, Zhou Y, Gourion B, Barbe V, Chang J, Cruveiller S, Dossat C, Gillett W, Gruffaz C, Haugen E, Hourcade E, Levy R, Mangenot S, Muller E, Nadalig T, Pagni M, Penny C, Peyraud R, Robinson DG, Roche D, Rouy Z, Saenampechek C, Salvignol G, Vallenet D, Wu Z, Marx CJ, Vorholt JA, Olson MV, Kaul R, Weissenbach J, Médigue C, Lidstrom ME (2009) *Methylobacterium* genome sequences: a reference blueprint to investigate microbial metabolism of C1 compounds from natural and industrial sources. PLoS One 4:e5584. https://doi.org/10.1371/journal.pone.0005584

Wang T, Guan C, Guo J, Liu B, Wu Y, Xie Z, Zhang C, Xing XH (2018) Pooled CRISPR interference screening enables genome-scale functional genomics study in bacteria with superior performance. Nat Commun 9:2475. https://doi.org/10.1038/s41467-018-04899-x

Wang T, Wang M, Zhang Q, Cao S, Li X, Qi Z, Tan Y, You Y, Bi Y, Song Y, Yang R, Du Z (2019) Reversible gene expression control in *Yersinia pestis* by using an optimized CRISPR interference system. Appl Environ Microbiol 85:e00097–e00019. https://doi.org/10.1128/AEM.00097-19

Westbrook AW, Ren X, Oh J, Moo-Young M, Chou CP (2018) Metabolic engineering to enhance heterologous production of hyaluronic acid in *Bacillus subtilis*. Metab Eng 47:401–413. https://doi.org/10.1016/j.ymben.2018.04.016

Woolston BM, Emerson DF, Currie DH, Stephanopoulos G (2018) Rediverting carbon flux in *Clostridium ljungdahlii* using CRISPR interference (CRISPRi). Metab Eng 48:243–253. https://doi.org/10.1016/j.ymben.2018.06.006

Yang YM, Chen WJ, Yang J, Zhou YM, Hu B, Zhang M, Zhu LP, Wang GY, Yang S (2017) Production of 3-hydroxypropionic acid in engineered *Methylobacterium extorquens* AM1 and its reassimilation through a reductive route. Microb Cell Factories 16:179. https://doi.org/10.1186/s12934-017-0798-2

Yang J, Zhang CT, Yuan XJ, Zhang M, Mo XH, Tan LL, Zhu LP, Chen WJ, Yao MD, Hu B, Yang S (2018) Metabolic engineering of *Methylobacterium extorquens* AM1 for the production of butadiene precursor. Microb Cell Factories 17:194. https://doi.org/10.1186/s12934-018-1042-4

Zhan Y, Xu Y, Zheng P, He M, Sun S, Wang D, Cai D, Ma X, Chen S (2019) Establishment and application of multiplexed CRISPR interference system in *Bacillus licheniformis*. Appl Microbiol Biotechnol 104:391–403. https://doi.org/10.1007/s00253-019-10230-5

Zhang M, Yuan XJ, Zhang C, Zhu LP, Mo XH, Chen WJ, Yang S (2019) Bioconversion of methanol into value-added chemicals in native and synthetic methylotrophs. Curr issues Mol biol 33:225–236. https://doi.org/10.21775/cimb.033.225